the plant journal

SEB SOCIETY FOR EXPERIMENTAL BIOLOGY

The Plant Journal (2021) **107,** 1346–1362 doi: 10.1111/tpj.15383

Karrikins control seedling photomorphogenesis and anthocyanin biosynthesis through a HY5-BBX transcriptional module

Katharina Bursch[1], Ella T. Niemann[1], David C. Nelson[2] and Henrik Johansson[1]*

[1]*Institute of Biology/Applied Genetics, Dahlem Centre of Plant Sciences (DCPS), Freie Universität Berlin, Berlin, 14195, Germany, and*

[2]*Department of Botany and Plant Sciences, University of California, Riverside, CA 92521, USA*

Received 22 February 2021; accepted 18 June 2021; published online 23 June 2021.
*For correspondence (e-mail a.h.johansson@fu-berlin.de).

SUMMARY

The butenolide molecule, karrikin (KAR), emerging in smoke of burned plant material, enhances light responses such as germination, inhibition of hypocotyl elongation, and anthocyanin accumulation in Arabidopsis. The KAR signaling pathway consists of KARRIKIN INSENSITIVE 2 (KAI2) and MORE AXILLARY GROWTH 2 (MAX2), which, upon activation, act in an SCF E3 ubiquitin ligase complex to target the downstream signaling components SUPPRESSOR OF MAX2 1 (SMAX1) and SMAX1-LIKE 2 (SMXL2) for degradation. How degradation of SMAX1 and SMXL2 is translated into growth responses remains unknown. Although light clearly influences the activity of KAR, the molecular connection between the two pathways is still poorly understood. Here, we demonstrate that the KAR signaling pathway promotes the activity of a transcriptional module consisting of ELONGATED HYPOCOTYL 5 (HY5), B-BOX DOMAIN PROTEIN 20 (BBX20), and BBX21. The *bbx20 bbx21* mutant is largely insensitive to treatment with KAR_2, similar to a *hy5* mutant, with regards to inhibition of hypocotyl elongation and anthocyanin accumulation. Detailed analysis of higher order mutants in combination with RNA-sequencing analysis revealed that anthocyanin accumulation downstream of SMAX1 and SMXL2 is fully dependent on the HY5-BBX module. However, the promotion of hypocotyl elongation by SMAX1 and SMXL2 is, in contrast to KAR_2 treatment, only partially dependent on BBX20, BBX21, and HY5. Taken together, these results suggest that light- and KAR-dependent signaling intersect at the HY5-BBX transcriptional module.

Keywords: ***Arabidopsis thaliana*, BBX proteins, HY5, karrikin, light signaling.**

INTRODUCTION

Karrikins (KARs) are a class of butenolide molecules found in the smoke of burned plant material that can induce germination of many plant species that emerge after fire (Dixon *et al.*, 2009; Flematti *et al.*, 2004; Nelson *et al.*, 2012). Intriguingly, KAR perception is widely conserved and not limited to fire-followers (Merritt *et al.*, 2006; Nelson *et al.*, 2012). For example, germination of dormant *Arabidopsis thaliana* seeds can be stimulated by KARs (Nelson *et al.*, 2009). Additionally, KAR treatment enhances responses of seedlings to light. These responses include inhibition of hypocotyl elongation, enhancement of cotyledon expansion, and transcriptional upregulation of light-responsive genes not only in Arabidopsis, but also in *Brassica tournefortii* (Nelson *et al.*, 2010; Sun *et al.*, 2020). Six KARs have been detected in smoke extracts (KAR_1 to KAR_6) (Flematti *et al.*, 2009; Hrdlička *et al.*, 2019), with KAR_2 being most potent in Arabidopsis, inducing responses at the nanomolar to micromolar range (Nelson *et al.*, 2010; Nelson *et al.*, 2009).

Many studies have aimed to understand how KARs affect plant growth by using Arabidopsis as a model system. KAR signaling is mediated by the α/β-hydrolase KARRIKIN INSENSITIVE 2 (KAI2)/HYPOSENSITIVE TO LIGHT (HTL), which acts as a receptor (Guo *et al.*, 2013; Sun and Ni, 2011; Waters *et al.*, 2012). Activation of KAI2 promotes its interaction with the F-box protein MORE AXILLARY GROWTH 2 (MAX2) (Toh *et al.*, 2014; Wang *et al.*, 2020). Both KAI2 and MAX2 are essential for KAR signaling. Arabidopsis *kai2* and *max2* mutants share many phenotypes, including increased primary seed dormancy (Nelson *et al.*, 2011; Waters *et al.*, 2012), an elongated hypocotyl (Nelson *et al.*, 2011; Waters *et al.*, 2012), reduced cotyledon size (Shen *et al.*, 2007; Sun and Ni, 2011), enhanced root skewing (Swarbreck *et al.*, 2019), and impaired root hair

© 2021 The Authors.
The Plant Journal published by Society for Experimental Biology and John Wiley & Sons Ltd.
This is an open access article under the terms of the Creative Commons Attribution License, which permits use, distribution and reproduction in any medium, provided the original work is properly cited.

development (Villaécija-Aguilar *et al.*, 2019). In rice, KAI2/DWARF14-LIKE (D14L) inhibits elongation of dark-grown mesocotyls (Zheng *et al.*, 2020) and is required for symbiosis with arbuscular mycorrhizal fungi (Choi *et al.*, 2020; Gutjahr *et al.*, 2015). The many developmental defects of KAR signaling mutants in the absence of KAR and the lack of evidence for KARs in living plants have led to the hypothesis that KAR mimics an endogenous signal named KAI2 ligand (KL) (Bythell-Douglas *et al.*, 2017; Conn and Nelson, 2015; Sun *et al.*, 2016; Waters *et al.*, 2012). As an F-box protein, MAX2 functions within an SCF (Skp1, Cullin, F-box) E3 ubiquitin ligase complex to polyubiquitinate specific proteins, targeting them for proteolysis (Stirnberg *et al.*, 2007). Mutations in the downstream signaling components *SUPPRESSOR OF MAX2 1* (*SMAX1*) and *SMAX1-LIKE 2* (*SMXL2*) completely suppress *max2* phenotypes at germination and early seedling stages, suggesting that they are the main inhibitors of KAR responses (Stanga *et al.*, 2016; Stanga *et al.*, 2013). Upon activation, the KAI2-SCF^{MAX2} complex targets SMAX1 and SMXL2 for degradation (Khosla *et al.*, 2020; Wang *et al.*, 2020).

The plant hormones auxin, jasmonate, and gibberellic acid also signal through SCF-mediated mechanisms. In auxin and jasmonate signaling, the Aux/IAA and JAZ proteins that are targeted for degradation act in complexes with transcription factors and TOPLESS (TPL)/TOPLESS-RELATED (TPR) transcriptional corepressors. Thus, hormone perception leads to a loss of transcriptional repression (Blázquez *et al.*, 2020). SMAX1 and SMXL2 may act similarly because they are nuclear-localized proteins that share a conserved EAR motif that recruits TPL/TPRs (Soundappan *et al.*, 2015; Wang *et al.*, 2020; Khosla *et al.*, 2020; Bennett and Leyser, 2014). The direct transcriptional targets of SMAX1 and SMXL2 and the identity of any transcription factor partner proteins remain unknown. Nonetheless, a number of genes that are transcriptionally regulated by KARs have been identified. The transcript levels of *DWARF14-LIKE2* (*DLK2*), *KARRIKIN UPREGULATED F-BOX1* (*KUF1*), and *B-BOX DOMAIN PROTEIN 20* (*BBX20*)/*SALT TOLERANCE HOMOLOG 7* (*STH7*)/*bzr1-1D SUPPRESSOR1* (*BZS1*) are particularly strongly and consistently upregulated by KARs and are often used as marker genes for KAR signaling (Nelson *et al.*, 2010; Nelson *et al.*, 2011; Scaffidi *et al.*, 2013; Waters *et al.*, 2012; Waters and Smith, 2013; Yao *et al.*, 2018). Consequently, the transcript levels of these genes are downregulated in the *kai2* and *max2* mutants (Nelson *et al.*, 2011; Waters *et al.*, 2012) and at least *DLK2* and *KUF1* are highly upregulated in the *smax1 smxl2* mutant (Stanga *et al.*, 2016).

Intriguingly, the KAR signaling pathway strongly resembles that of the most recently identified plant hormone, strigolactone (SL) (Gomez-Roldan *et al.*, 2008; Umehara *et al.*, 2008). Also comprising butenolide-containing compounds, SLs are perceived by the α/β-hydrolase DWARF 14 (D14), a homolog of KAI2 (Waters *et al.*, 2012). Upon SL perception, D14 interacts with SCF^{MAX2} and targets SMXL6, SMXL7, and SMXL8 (orthologs of DWARF53 in rice) for degradation (Jiang *et al.*, 2013; Soundappan *et al.*, 2015; Wang *et al.*, 2015; Yao *et al.*, 2016; Zhou *et al.*, 2013). Hence, KAR and SL signal through MAX2-dependent pathways that use homologous receptor proteins to target different sets of homologous target proteins. Although the KAR downstream signaling component SMXL2 can be targeted by SL signaling (Wang *et al.*, 2020), these are two largely distinct pathways (Waters *et al.*, 2015; Soundappan *et al.*, 2015). It is important to note that many studies investigating the SL signaling pathway have relied on the use of the synthetic SL-analog GR24 as a racemic mixture (*rac*-GR24). The two enantiomers that compose *rac*-GR24, $GR24^{5DS}$ and $GR24^{ent\text{-}5DS}$, primarily activate D14- and KAI2-dependent signaling, respectively (Scaffidi *et al.*, 2014). Hence, it is likely that some effects of *rac*-GR24 that have been attributed as SL pathway responses in the literature are in fact mediated by the KAR pathway.

Interestingly, *KAI2* was first identified as *HTL* as a result of the elongated hypocotyl phenotype of the *htl* mutant (Sun and Ni, 2011). Mutants of *MAX2* display a similar phenotype, whereas the *smax1 smxl2* double mutant shows strong suppression of hypocotyl elongation. This suggests a close connection between KAR and light signaling (Nelson *et al.*, 2011; Shen *et al.*, 2007; Stanga *et al.*, 2016; Stanga *et al.*, 2013). Indeed, there is significant overlap between KAR-induced genes and light-responsive transcripts (Nelson *et al.*, 2010). In addition, a mutant of the bZIP transcription factor HY5, a key positive regulator of photomorphogenesis, shows a strongly reduced inhibition of hypocotyl elongation when treated with KAR. This suggests that HY5 activity is important for this response (Nelson *et al.*, 2010). Furthermore, KAR-induced inhibition of hypocotyl elongation is dependent on the presence of light (Nelson *et al.*, 2010). This light requirement can be overcome by mutation of the E3 ubiquitin ligase CONSTITUTIVELY PHOTOMORPHOGENIC 1 (COP1) (Jia *et al.*, 2014). However, light and HY5 are not essential for KAR perception or many KAR-induced transcriptional responses (Nelson *et al.*, 2010; Waters and Smith, 2013), suggesting that HY5 represents a downstream point of convergence between light and KAR signaling.

As a major positive regulator of photomorphogenesis in Arabidopsis, HY5 is negatively regulated by the COP1/SUPPRESSOR OF PHYA-105 (SPA) E3 ubiquitin ligase complex in darkness and accumulates in correlation with the surrounding light intensity (Osterlund *et al.*, 2000). Its function as a DNA-binding transcriptional regulator without any apparent transactivation domain suggests that HY5 requires partner proteins to induce transcription of its direct targets (Oyama *et al.*, 1997; Burko *et al.*, 2020; Ang *et al.*, 1998). Within the Arabidopsis BBX zinc finger family

© 2021 The Authors.
The Plant Journal published by Society for Experimental Biology and John Wiley & Sons Ltd.,

of transcription factors, BBX20 to BBX23 belong to structural group IV. These proteins form a unique cluster within group IV that interact with HY5 and positively regulate photomorphogenesis (Chang *et al.*, 2008; Datta *et al.*, 2008; Fan *et al.*, 2012; Khanna *et al.*, 2009; Zhang *et al.*, 2017). Similar to HY5, these BBX proteins are negatively regulated by the COP1/SPA complex in darkness and hence accumulate in response to light (Chang *et al.*, 2011; Fan *et al.*, 2012; Xu *et al.*, 2016; Zhang *et al.*, 2017). Recent work suggests that BBX20 to BBX23 fulfill the role of cofactors of HY5, allowing for HY5-dependent transcriptional regulation, induction of photomorphogenic growth, and anthocyanin accumulation (Bursch *et al.*, 2020; Zhang *et al.*, 2017). The strong transcriptional induction of *BBX20* in response to KAR (Nelson *et al.*, 2010) suggests that BBX20 could also play a role in KAR responses. Indeed, transgenic lines overexpressing a BBX20-SRDX fusion protein, which causes dominant-negative transcriptional repression, are hyposensitive to KAR_1 and *rac*-GR24 treatment (Thussagunpanit *et al.*, 2017; Wei *et al.*, 2016). It is difficult to attribute the specific role of *BBX20* versus its homologs in these responses, however, based on experiments that have used dominant-negative fusion proteins or overexpression.

Although the core KAR signaling mechanism, consisting of KAI2-SCF^{MAX2}-mediated degradation of SMAX1 and SMXL2, is well described, it is not known how SMXL degradation leads to downstream growth responses. In the present study, we analyse the role of BBX20 in the KAR signaling pathway through both chemical and genetic approaches using knockout mutants. We find that BBX20 and its close homolog BBX21 are essential for KAR-induced inhibition of hypocotyl elongation and anthocyanin accumulation. Our detailed genetic analysis suggests that BBX20 and BBX21 act in a HY5-dependent transcriptional module downstream of SMAX1 and SMXL2. RNA-sequencing (RNA-seq) analysis reveals large-scale transcriptional changes in the *smax1 smxl2* mutant, and we show that BBX20 and BBX21 are required for a subset of SMAX1/SMXL2-dependent transcriptional regulation. Overall, our data imply that the KAR signaling pathway promotes the activity of the HY5-BBX module and that this module represents a point of convergence between KAR and light signaling.

RESULTS

BBX20 expression is inhibited by SMAX1 and SMXL2

BBX20/STH7/BZS1 is frequently used as a transcriptional reporter for KAR-induced signaling because *BBX20* transcript levels are promoted by KAR_1 or KAR_2 treatment in both seeds and young seedlings (Nelson *et al.*, 2010; Scaffidi *et al.*, 2013; Waters *et al.*, 2012; Waters and Smith, 2013; Yao *et al.*, 2018). Accordingly, *BBX20* transcript levels are reduced in *kai2* and *max2* mutants, which are unable to perceive KARs or putatively KL (Nelson *et al.*, 2011; Waters *et al.*, 2012). Similar to these previous reports, we observed a 1.5-fold increase in *BBX20* transcript levels in Arabidopsis seedlings grown for 4 days in constant red light on medium supplemented with 1 μM KAR_2 compared to seedlings grown on medium containing 0.1% (v/v) acetone (control) (Figure 1a). Correspondingly, we observed a two-fold reduction of *BBX20* transcript levels in the *kai2* and *max2* mutants as described previously (Figure 1b) (Nelson *et al.*, 2011; Waters *et al.*, 2012). By contrast, *BBX20* transcript levels were upregulated by more than three-fold in the *smax1 smxl2* mutant (Figure 1b). This is consistent with the proposed role of *SMAX1* and *SMXL2* as inhibitors of KAR/KL responses that are targeted for degradation by KAI2-SCF^{MAX2} (Khosla *et al.*, 2020; Wang *et al.*, 2020; Stanga *et al.*, 2016).

To examine tissue-specific changes of *BBX20* expression in response to KAR_2 treatment, we created two independent *pBBX20::GUS-GFP* transcriptional reporter lines in *A. thaliana*. We analyzed GUS expression in seedlings from these lines grown in red light for 24, 48 and 96 h after the induction of germination on medium with or without 1 μM KAR_2 (Figure 1c-t). Under control conditions, the promoter activity of *BBX20* was most strongly observed in the roots of seedlings at all timepoints (Figure 1c,d,f). This was consistent with previous observations of *BZS1::GUS* activity in the roots of light- and dark-grown seedlings (Fan *et al.*, 2012). More specifically, the promoter of *BBX20* was active in the differentiation zone of developing seedlings (Figure 1e,h). At 96 h, GUS expression was also evident in the shoot apical meristematic region (Figure 1g). In line with the results from the quantitative reverse transcriptase (qRT)-PCR analysis (Figure 1a), treatment with KAR_2 enhanced the activity of the transcriptional reporter (Figure 1i-n). Next, we introgressed the reporter transgene into the *smax1 smxl2* background. This also resulted in increased *BBX20* promoter activity in the roots and the shoot apical meristem (Figure 1o-t). Additionally, GUS expression was increased in the cotyledons and the hypocotyl of KAR_2-treated seedlings and *smax1 smxl2* seedlings by 24 h (Figure 1i,o). A second transgenic line produced similar results, although with lower GUS expression overall (Figure S1a-l). Although these experiments did not reveal any GUS staining of the hypocotyl and cotyledons in 4-day-old seedlings, further analysis of *BBX20* transcript levels via qRT-PCR in dissected cotyledons and hypocotyls revealed that *BBX20* is also induced by KAR_2 in these tissues after 96 h (Figure S1m). Regardless, although the activity of the *BBX20* promoter was increased in response to KAR_2 treatment or loss of *SMAX1* and *SMXL2*, it remained restricted to the same tissues. This implies that the spatial distribution of *BBX20* expression in seedlings is not limited by the KAR/KL pathway.

© 2021 The Authors.

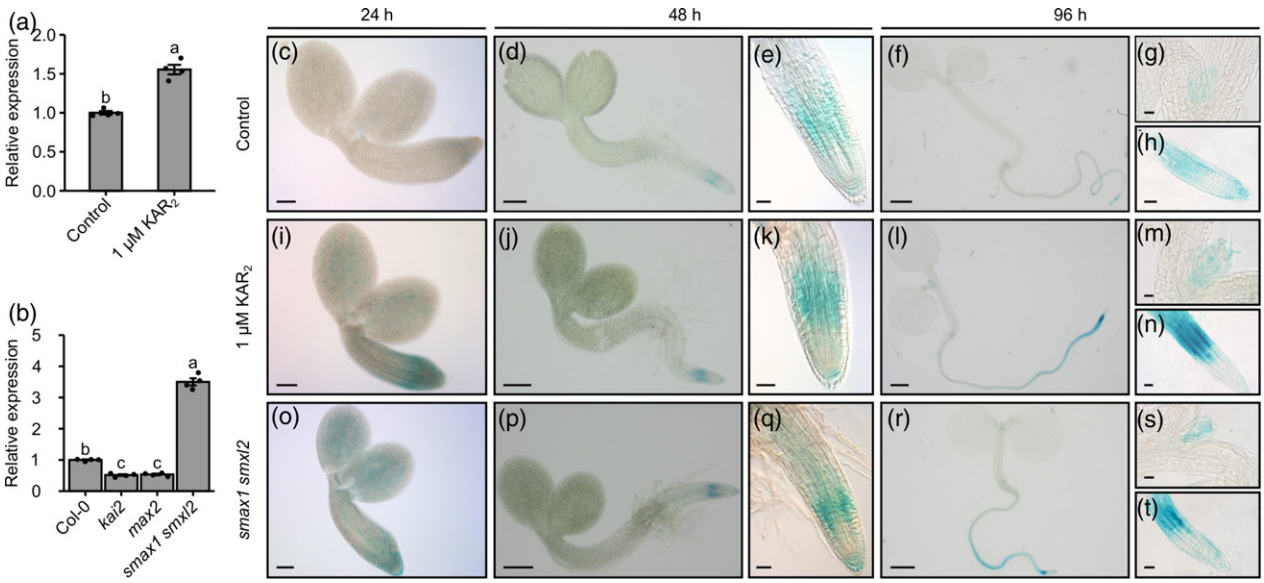

Figure 1. *BBX20* expression is promoted by KAR downstream of SMAX1 and SMXL2.
(a, b) Transcript abundance of *BBX20* relative to *GADPH* and *TFIID* reference genes in 4-day-old seedlings grown in 80 μmol m^{-2} sec^{-1} red light treated with 0.1% acetone (control) or 1 μM KAR_2 (a) or without supplements (b) (n = 4 independent biological replicates represented by black dots). Bars represent the mean and error bars represent the SE. Different letters denote statistically significant differences as determined by a two-sample t-test ($P < 0.05$) (a) or one-way ANOVA followed by Tukey's *post hoc* test ($P < 0.05$) (b). (c–t) GUS-staining of *pBBX20::GUS-GFP* line #1 grown for 24, 48 or 96 h in 80 μmol m^{-2} sec^{-1} red light. In (c) to (h) and (o) to (t), the seeds were grown on control medium (containing 0.1% acetone). In (j) to (o), the seeds were grown on medium containing 1 μM KAR_2. Scale bars = 50 μM (c, e, g, h, i, j, k, m, n, o, q, s, t), 200 μM (d, j, p), and 500 μM (f, l, r).

BBX20 is partially required for KAR-induced inhibition of hypocotyl elongation

Although the positive regulation of *BBX20* transcript levels by KAR treatment has long been known (Nelson *et al.*, 2010), a lack of available T-DNA insertion mutant alleles for *BBX20* has limited genetic evaluation of its potential physiological role in KAR signaling. Because we had recently generated a loss-of-function allele of *BBX20* with clustered regularly interspaced short palindromic repeats (CRISPR)-CRISPR-associated protein 9 (Cas9) (Bursch *et al.*, 2020), we set out to investigate whether KAR signaling is impaired in this mutant. In line with previous observations, increasing concentrations of KAR_2 resulted in progressively stronger inhibition of hypocotyl elongation in wild-type (WT) Col-0 seedlings grown in constant red light (Figure 2b and Figure S2a) (Nelson *et al.*, 2010). The *bbx20-1* mutant, which has an elongated hypocotyl compared to WT (Bursch *et al.*, 2020), also showed inhibition of hypocotyl elongation in response to KAR_2 treatment (Figure S2a). However, analysis of the effect of KAR_2 treatment relative to control conditions for each genotype revealed that the *bbx20-1* mutant is partially insensitive to the KAR_2 treatment (Figure 2a,b). We investigated whether the different effects of KAR_2 on WT and *bbx20-1* seedling growth are the result of different germination rates in our conditions. No significant difference was observed between the two genotypes or treatments in the first 3 days of growth, suggesting that KAR_2 has minimal effects on germination in these conditions (Figure S2c). In order to verify the reduced KAR_2 sensitivity of *bbx20*, we additionally created a *bbx20-2* mutant in the Landsberg *erecta* ecotype (L*er*), using CRISPR-Cas9 as described previously (Bursch *et al.*, 2020). We identified a frameshift allele with the same 1-bp deletion as in the Col-0 background (*bbx20-1*) resulting in an early stop codon (Bursch *et al.*, 2020). Similar to *bbx20-1*, *bbx20-2* seedlings had elongated hypocotyls compared to WT (L*er*) and reduced sensitivity to KAR_2 (Figure 2c,d and Figure S2b). These data suggest that the transcriptional induction of *BBX20* by KAR is a component of growth responses to KAR in seedlings.

BBX20 and BBX21 act redundantly to inhibit hypocotyl elongation in response to KAR

BBX20 belongs to structural group IV of the Arabidopsis BBX proteins, showing the highest sequence homology to BBX21/STH2, BBX22/LZF1/STH3, and BBX23 (Khanna *et al.*, 2009), which all positively regulate photomorphogenesis (Datta *et al.*, 2007; Datta *et al.*, 2008; Zhang *et al.*, 2017). Previous studies have indicated that these factors can act redundantly (Bursch *et al.*, 2020; Datta *et al.*, 2008; Zhang *et al.*, 2017). Therefore, we investigated whether other BBX proteins are involved in KAR-induced inhibition of hypocotyl elongation by testing the *bbx20-1 (bbx20)*, *bbx21-1 (bbx21)*, *bbx22-1 (bbx22)*, and *bbx23-1 (bbx23)* single mutants. Analysis of the average KAR_2 response of three

© 2021 The Authors.

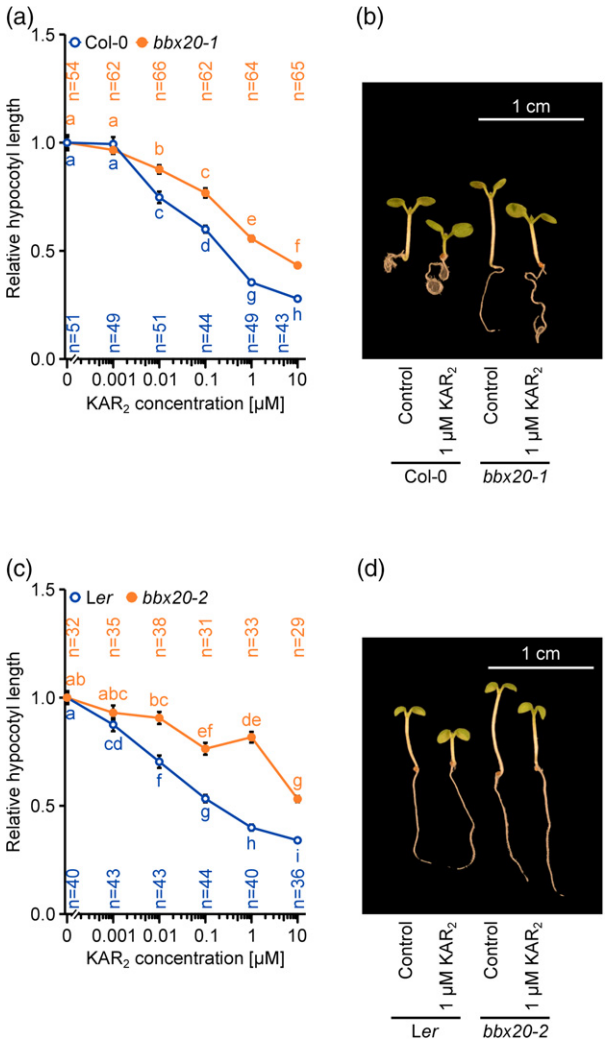

Figure 2. The *bbx20* mutant is hyposensitive to KAR_2 treatment.
(a) Hypocotyl measurements of Col-0 and *bbx20-1* mutant seedlings grown for 5 days on ½ MS medium supplemented with different concentrations of KAR_2 in 70 µmol m^{-2} sec^{-1} red light. The data is shown as relative to control (0 µM KAR_2) within each genotype. (b) Representative image of seedlings grown as in (a). (c) Hypocotyl measurements of L*er* and *bbx20-2* mutant seedlings grown and analyzed as in (a). For (a) and (c), error bars represent the SE and different letters denote statistically significant differences as determined by a pairwise Wilcoxon rank sum test ($P < 0.05$). (d) Representative image of seedlings grown as in (c).

independent experiments revealed that, in addition to the *bbx20* mutants, *bbx21* showed a small reduction of the KAR_2 response (29% and 44% inhibition of hypocotyl elongation, respectively, versus 57% for WT) (Figure 3a,d). By contrast, the *bbx22* and *bbx23* mutants showed a response to KAR_2 that was similar to WT, with 50% and 53% growth inhibition, respectively. This suggests that *BBX22* and *BBX23* do not play a role in KAR responses. However, because functional redundancy might mask the role of individual BBX proteins, we tested higher order mutants. Strikingly, we observed a strongly reduced KAR_2 response in the *bbx20-1 bbx21-1* (*bbx2021*) double mutant (Figure 3b,e). To verify these results, we created a *bbx20-2 bbx21-2* double mutant in the L*er* background. We observed a similar reduction in KAR_2 response in this independent double mutant (Figure S3). This suggests that *BBX20* and *BBX21* have essential, partially redundant roles in mediating inhibition of hypocotyl elongation in response to KAR_2.

Functional redundancy in the regulation of hypocotyl elongation has also been shown for *BBX22* and *BBX23* (Zhang *et al.*, 2017). However, although we used the same mutant alleles as studied previously, in our conditions the *bbx22-1 bbx23-1* (*bbx2223*) double mutant showed a hypocotyl length and response to KAR_2 treatment similar to WT (Figure 3c,f). Additionally, we observed little difference in the KAR_2 response of *bbx20-1 bbx21-1 bbx22-1 bbx23-1* (*bbx20212223*) seedlings compared to *bbx2021* (Figure 3c, f). This comprehensive genetic analysis of single and higher order *bbx* mutants suggests that *BBX22* and *BBX23* do not contribute to KAR_2-dependent growth responses in light-grown seedlings.

bbx20 and *bbx21* partially suppress the *smax1 smxl2* mutant phenotype in seedlings

BBX20 transcript levels have an inverse relationship with the hypocotyl length of the *kai2*, *max2* and *smax1 smxl2* mutants (Figure 1b) (Nelson *et al.*, 2011; Stanga *et al.*, 2016; Waters *et al.*, 2012). Our data also suggest that *BBX20* and *BBX21* are essential for KAR-induced inhibition of hypocotyl elongation. Therefore, we hypothesized that altered BBX activity could account for at least some phenotypes of KAR pathway mutants. To test this, we first analyzed the genetic relationship between *bbx2021* and the *smax1 smxl2* double mutant. The *smax1 smxl2* double mutant has strongly reduced hypocotyl elongation compared to WT in accordance with a constitutively active KAR/KL signaling pathway (Figure 4) (Stanga *et al.*, 2016). Under the proposed hypothesis, the short hypocotyl phenotype of *smax1 smxl2* could be a result of increased BBX20/21 activity. We observed a hypocotyl elongation phenotype for the *smax1 smxl2 bbx2021* quadruple mutant that was between the extremes of *smax1 smxl2* and *bbx2021* (Figure 4). A conservative interpretation of this result is that SMAX1/SMXL2 and BBX20/21 affect hypocotyl elongation through independent pathways that have additive effects. Alternatively, it may signify a partial epistatic interaction as a result of functional redundancy (e.g. BBX20 and BBX21 are not the only proteins that act downstream of SMAX1 and SMXL2 to control hypocotyl elongation). Indeed, the relative phenotype of the *bbx2021* mutant was enhanced in the *smax1 smxl2* mutant background (approximately 60% and 320% longer compared to WT and *smax1 smxl2*, respectively) (Figure 4). Also considering the transcriptional regulation of *BBX20* by KAR/KL signaling and the reduced response to KAR in *bbx2021*, we

© 2021 The Authors.

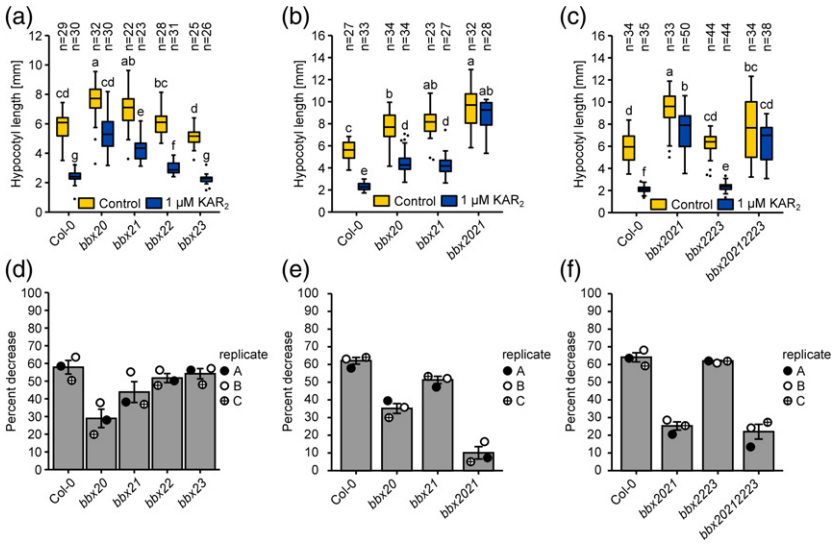

Figure 3. *BBX20* acts together with *BBX21* to inhibit hypocotyl elongation in response to KAR.
(a – c) Hypocotyl measurements of seedlings grown for 5 days on ½ MS medium containing 0.1% acetone (control) or 1 µM Kar_2 in 70 µol m^{-2} sec^{-1} red light. Box plots represent medians and interquartile ranges with whiskers extending to the largest/smallest value within the 1.5 × interquartile range and outliers are shown as dots. Different letters denote statistically significant differences as determined by two-way ANOVA followed by Tukey's test (a, b) or a Wilcoxon rank sum test (c) ($P < 0.05$). (d–f) Average percentage decrease of hypocotyl length in response to KAR treatment in three individual experiments corresponding to (a) to (c). Bars represent the mean and error bars represent the SE. Replicate A corresponds to the data shown in (a) to (c).

favor the interpretation that BBX20 and BBX21 are acting downstream of SMAX1 and SMXL2. In line with the stronger phenotype of *bbx20* compared to *bbx21* when treated with KAR_2 (Figure 3a,b), the *smax1 smxl2* phenotype was more strongly suppressed by *bbx20* than by *bbx21* (Figure 4).

Next, we analyzed the genetic relationship between *bbx2021*, *kai2*, and *max2*, respectively. Consistent with previous studies, *kai2* and *max2* showed a long hypocotyl phenotype when grown in constant red light for 5 days (Shen *et al.*, 2007; Sun and Ni, 2011) (Figure S4a,b). Analysis of the *kai2 bbx2021* and the *max2 bbx2021* triple mutants revealed significantly longer hypocotyls than either *kai2*, *max2*, or *bbx2021*. This additive phenotype further suggests that, if BBX20 and BBX21 regulate hypocotyl growth downstream of SMAX1 and SMXL2, they are not the only proteins to do so.

BBX20 and *BBX21* promote anthocyanin biosynthesis downstream of *SMAX1* and *SMXL2*

To further investigate the genetic interaction of *BBX20/21* and *SMAX1/SMXL2*, we performed an RNA-seq analysis of *bbx2021* and *smax1 smxl2* seedlings grown for 4 days in red light. We defined differentially expressed genes (DEGs) as those with an absolute fold change of 1.5-fold or more in the mutant compared to WT, with Bonferroni adjusted $P \leq 0.05$. We identified 2635 genes that were differentially expressed in the *smax1 smxl2* mutant. By contrast, only 111 genes were misregulated in the *bbx2021* mutant compared to WT (Data S1). A comparison of both sets of DEGs showed a statistically significant overlap of 48 genes (Fisher's exact test, $P < 0.05$) (Figure 5a and Table S1). Consistent with the opposing roles of these factors in the regulation of hypocotyl elongation, approximately 90% of these overlapping DEGs were oppositely regulated in *bbx2021* and *smax1 smxl2* (Figure 5b). Gene Ontology (GO)-term analysis of these overlapping genes revealed an enrichment in genes known to be involved in the flavonoid biosynthetic process and glucosinolate catabolic process, as well as genes known to be regulated in response to UV-B and karrikin (Figure 5c). qRT-PCR analysis of two genes classified as "responsive to karrikin" (*BIC1* and *ABCI20*) confirmed that their transcript levels were reduced in *bbx2021* and elevated in *smax1 smxl2*. Furthermore, the elevated expression of *BIC1* and *ABCI20* in the *smax1 smxl2* mutant was completely suppressed by *bbx2021* in the *smax1 smxl2 bbx2021* quadruple mutant (Figure 5d,e). This suggests that the KAR-induced regulation of these transcripts is fully dependent on BBX20 and BBX21.

The GO-term analysis revealed 'flavonoid biosynthetic process' as the most enriched GO-term in the overlap of DEGs from *bbx2021* and *smax1 smxl2* (Figure 5c). qRT-PCR analysis of genes from this GO-term confirmed the low and high transcript levels of *FLS1*, *F3H*, *MYB12*, and *CHS* in *bbx2021* and *smax1 smxl2*, respectively. Similar to the regulation of *BIC1* and *ABCI20*, analysis of the *smax1 smxl2 bbx2021* quadruple mutant showed that *bbx2021* is epistatic to *smax1 smxl2* in the regulation of these genes (Figure 5f-i). This suggests that BBX20 and BBX21 act downstream of SMAX1 and SMXL2 to promote flavonoid biosynthesis and led us to test whether the induction of anthocyanin accumulation by KAR is dependent on BBX20 and BBX21. KAR treatment has previously been shown to induce anthocyanin accumulation in WT seedlings associated with a *KAI2*-dependent transcriptional induction of the flavonoid biosynthesis gene *CHS* (Thussagunpanit *et al.*, 2017; Waters and Smith, 2013). In line with these reports, we observed increased anthocyanin accumulation in WT seedlings after a 1 µM KAR_2 treatment that was dependent on KAI2 (Figure 5j). Consistent with earlier reports,

© 2021 The Authors.

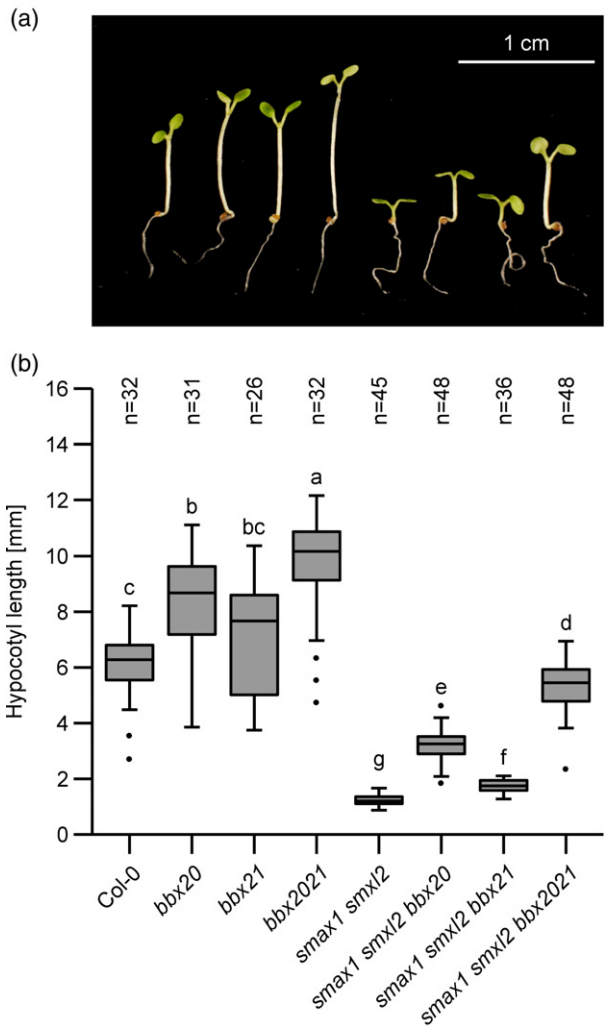

Figure 4. *bbx20* and *bbx21* partially suppress the *smax1 smxl2* mutant phenotype.
(a) Representative picture of 5-day-old seedlings grown in 70 μmol m^{-2} sec^{-1} red light. (b) Hypocotyl measurements of seedlings grown as in (a). Box plots represent medians and interquartile ranges with whiskers extending to the largest/smallest value within the 1.5 × interquartile range and outliers are shown as dots. Different letters denote statistically significant differences as determined by the Welch test followed by a Wilcoxon test ($P < 0.05$).

bbx2021 seedlings accumulated less anthocyanin under control conditions compared to WT (Figure 5j) (Bursch *et al.*, 2020; Datta *et al.*, 2007). Strikingly however, the *bbx2021* seedlings did not accumulate higher levels of anthocyanins in response to the KAR_2 treatment, suggesting that BBX20 and BBX21 are important regulators of KAR-induced anthocyanin accumulation that act downstream of SMAX1 and SMXL2 (Figure 5j). Supporting this idea, we observed that anthocyanin levels were increased by more than 2.5-fold in *smax1 smxl2* seedlings (Figure 5k). This phenotype was completely suppressed by *bbx2021* in the *smax1 smxl2 bbx2021* quadruple mutant (Figure 5k).

We observed that mutation of *SMAX1* and *SMXL2* had led to widespread changes in transcript abundance (Figure 5a). GO-term analysis of the 2635 DEGs revealed that, besides the impact on known KAR-responsive genes that had been identified in seeds, *smax1 smxl2* DEGs were enriched for genes involved in processes related to photosynthesis and translation (Figure S5a). To identify new genes that are most likely to be regulated by the KAR signaling pathway, we compared our *smax1 smxl2* data with publicly available transcriptome datasets from *kai2* and *max2* mutants (Li *et al.*, 2017; Van Ha *et al.*, 2014). Although these studies used different experimental conditions, we found an overlap of 41 genes among the three datasets (Figure S5b and Table S2). In line with the antagonistic roles of KAI2 or MAX2 and SMAX1/SMXL2, 38 of those genes had opposite differential expression patterns in *smax1 smxl2* compared to *kai2* and *max2* (Figure S5c). These putative KAR target genes included the often-used marker genes *KUF1*, *DLK2*, and *BBX20*. Interestingly, we identified a set of auxin-responsive genes that are suppressed by the KAR signaling pathway (Figure S5c). This list also contained *SMXL2*, suggesting that its transcript levels are promoted by KAR signaling, but the elevated expression of *SMXL2* in the *smax1 smxl2* mutant is likely an effect of the T-DNA insertion in *smxl2* as described previously (Stanga *et al.*, 2016). It is notable that, although BBX20 and BBX21 regulate a subset of the putative SMAX1/SMXL2 target genes, most of the genes appear to be regulated independently of BBX20/BBX21. Accordingly, qRT-PCR showed that expression of *KUF1*, *DLK2*, and *AT3G60290* was unaffected in *bbx2021* seedlings and was not significantly different from *smax1 smxl2* in the *smax1 smxl2 bbx2021* quadruple mutant (Figure S5d–f).

BBX20/21 and HY5 act together in KAR-induced inhibition of hypocotyl elongation

Similar to *bbx2021*, the inhibition of hypocotyl elongation by KAR is highly reduced in a *hy5* mutant (Nelson *et al.*, 2010; Waters and Smith, 2013). Although *HY5* expression was not changed in the *smax1 smxl2* mutant under our conditions (Data S1), the transcript levels of *HY5* have previously been shown to be elevated in response to KAR (Nelson *et al.*, 2010). Furthermore, *rac*-GR24 has been shown to promote HY5 protein stability in a MAX2-dependent manner (Tsuchiya *et al.*, 2010). We recently demonstrated that BBX20 and BBX21, together with BBX22, act as essential cofactors of HY5 in promoting photomorphogenesis (Bursch *et al.*, 2020). Therefore, we considered whether HY5, BBX20, and BBX21 act together to regulate the hypocotyl elongation response to KAR. Alternatively, because the *bbx2021* mutant did not fully suppress the *smax1 smxl2* short hypocotyl phenotype

© 2021 The Authors.

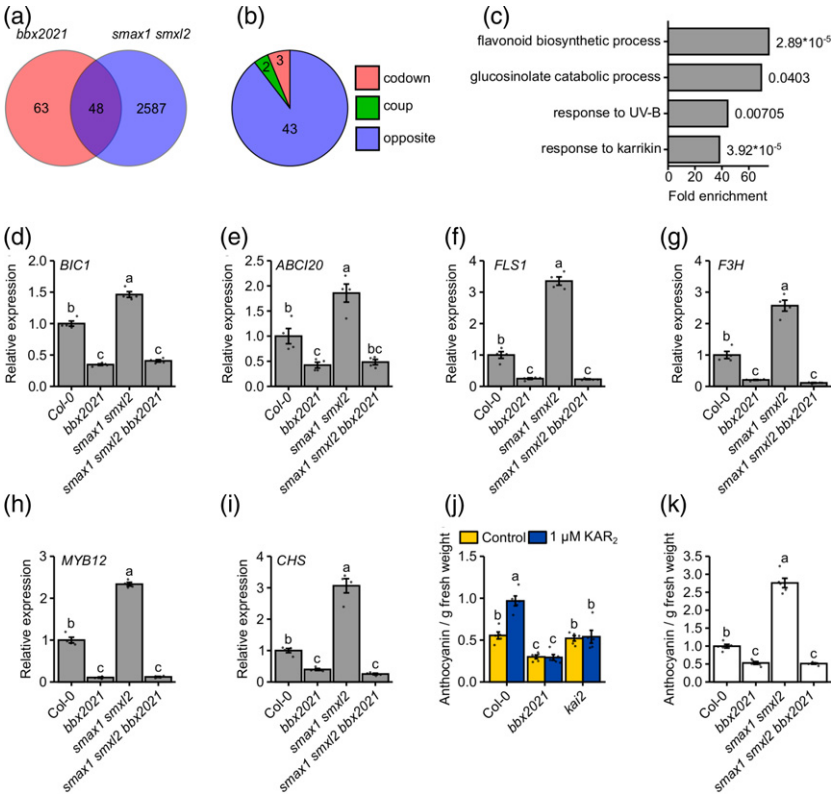

Figure 5. *BBX20* and *BBX21* promote anthocyanin biosynthesis downstream of *SMAX1* and *SMXL2*.
(a) Venn diagram showing the overlap between DEGs in *bbx2021* and *smax1 smxl2* from 4-day-old seedlings grown in 80 μmol m^{-2} sec^{-1} of red light. (b) Pie chart indicating coregulation of genes between the *bbx2021* and *smax1 smxl2* mutants. (c) GO analysis of the DEGs from the *bbx2021* and *smax1 smxl2* overlap in (a). (d–i) Transcript abundance of *BIC1* (d), *ABCI20* (e), *FLS1* (f), *F3H* (g), *MYB12* (h), and *CHS* (i) relative to *GADPH* and *TFIID* reference genes in 4-day-old seedlings grown in 80 μmol m^{-2} sec^{-1} red light ($n = 4$ independent biological replicates indicated by black dots). Bars represent the mean and error bars represent the SE. Different letters denote statistically significant differences as determined by one-way ANOVA followed by Tukey's *post hoc* test ($P < 0.05$). (j–k) Anthocyanin measurements of 4-day-old seedlings grown in 80 μmol m^{-2} sec^{-1} red light on medium containing 0.1% acetone (control) or 1 μM KAR_2 (j) or without supplements (k) ($n = 5$ independent biological replicates represented by black dots). Bars represent the mean and error bars represent SE and different letters denote statistically significant differences as determined by the Welch test followed by a Wilcoxon test ($P < 0.05$) (j) or by one-way ANOVA followed by Tukey's *post hoc* test ($P < 0.05$) (k).

(Figure 4b), HY5 might represent a second pathway that regulates hypocotyl elongation downstream of SMAX1 and SMXL2 in parallel to BBX20 and BBX21. To distinguish these possibilities, we first analyzed the KAR-induced inhibition of hypocotyl elongation of *bbx2021*, *hy5,* and the *hy5 bbx2021* triple mutant (Figure 6a). Similar to the *bbx202122* triple mutant, *bbx2021* displayed a long hypocotyl phenotype similar to *hy5* when grown under control conditions (Bursch *et al.*, 2020) and the *hy5 bbx2021* triple mutant showed no additional phenotype compared to *bbx2021* and *hy5* (Figure 6a). All of these mutants were largely insensitive to the KAR_2 treatment (Figure 6a), consistent with the hypothesis that BBX proteins and HY5 act together with respect to regulating hypocotyl elongation. However, this does not rule out the possibility of parallel pathways because a further reduction of the KAR response would be difficult to observe.

To resolve this genetic relationship, we created *smax1 smxl2 hy5* and *smax1 smxl2 hy5 bbx2021* mutants. Although *hy5* counteracted the short hypocotyl phenotype of *smax1 smxl2*, the *smax1 smxl2 hy5* triple mutant was not as long as *hy5*. However, mutation of *hy5* in WT led to an increase in hypocotyl length by 110%, whereas, in *smax1 smxl2*, the hypocotyl length was increased by 470% (Figure 6b). This suggests enhanced HY5 activity makes an important contribution to the phenotype of *smax1 smxl2*. In addition, hypocotyl elongation of *smax1 smxl2 hy5* was not further increased by the addition of *bbx2021* (Figure 6b). This result is consistent with a functional HY5-BBX20/BBX21 module acting downstream of SMAX1 and SMXL2 to partially suppress hypocotyl elongation. However, the *hy5* mutation had a stronger counteracting effect on *smax1 smxl2* hypocotyl elongation than *bbx2021*, implying that HY5 may rely on cofactors in addition to BBX20 and BBX21 to regulate hypocotyl elongation under these conditions. Hence, we hypothesized that there might be a role for BBX22 and BBX23 in the KAR signaling pathway as partners of HY5 that we were unable to detect with the chemical approach (Figure 3a,c). However, a *smax1 smxl2 bbx202122223* mutant did not show additional suppression of the *smax1 smxl2* phenotype compared to *smax1 smxl2 bbx2021* (Figure 6c). This supports our earlier conclusion that BBX20 and BBX21, but not BBX22 and BBX23, are involved in KAR-induced inhibition of hypocotyl elongation.

We noted that, although *hy5* strongly counteracted the *smax1 smxl2* phenotype, it was not complete suppression. This suggests that factors additional to HY5 act downstream of SMAX1 and SMXL2 to inhibit hypocotyl elongation. We reasoned that HY5-HOMOLOG (HYH), which can function redundantly with *HY5* in regulating hypocotyl elongation (Holm *et al.*, 2002), might also regulate hypocotyl elongation downstream of SMAX1 and SMXL2. To test this hypothesis, we created and analyzed the *smax1 smxl2*

© 2021 The Authors.

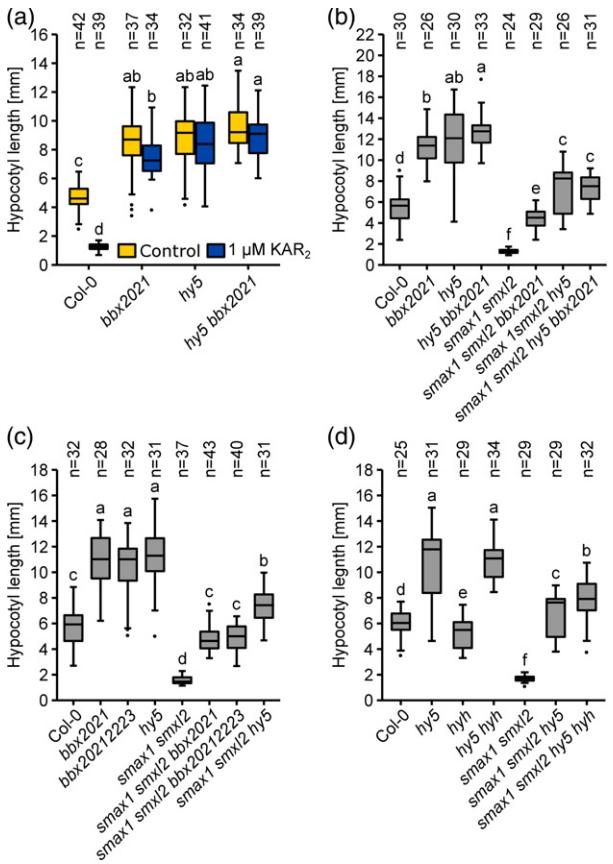

Figure 6. *bbx2021*-dependent suppression of the *smax1 smxl2* phenotype requires *HY5*.

(a–d) Hypocotyl measurements of 5-day-old seedlings grown in 70 µmol m^{-2} sec^{-1} red light. The seedlings were grown on medium containing 0.1% acetone (control) or 1 µM KAR_2 (a) or on medium without supplements (b–d). Box plots represent medians and interquartile ranges with whiskers extending to the largest/smallest value within the 1.5 × interquartile range and outliers are shown as dots. Different letters denote statistically significant differences as determined by one-way ANOVA followed by Tukey's test (a, c) or as determined by the Welch test followed by a Wilcoxon test (b, d) ($P < 0.05$).

hy5 hyh mutant. Interestingly, the addition of *hyh* resulted in further suppression of the *smax1 smxl2 hy5* phenotype (Figure 6d), suggesting that HYH also plays a role in suppressing hypocotyl elongation after activation of the KAR signaling pathway. However, the hypocotyl length of the quadruple mutant was still shorter than that of *hy5 hyh*, and so other players may yet be found. Taken together, these data indicate that HY5 and HYH, together with BBX20 and BBX21, partly regulate hypocotyl elongation downstream of SMAX1 and SMXL2.

The HY5-BBX20/21 module promotes anthocyanin accumulation downstream of SMAX1 and SMXL2

Consistent with the functional interdependence of HY5 and BBX20, BBX21, and BBX22 in the regulation of gene expression (Bursch *et al.*, 2020), evidence for HY5 regulation of most of the 44 genes coregulated by BBX20/21 and SMAX1/SMXL2 (Figure 5a) can be found in publicly available transcriptomic datasets (Table S1) (Bursch *et al.*, 2020; Zhao *et al.*, 2019). We observed similarly reduced expression of *BIC1*, *ABCI20*, *FLS1*, *F3H*, *MYB12*, and *CHS* in the *hy5* mutant as in *bbx2021*, and no additional changes in expression were observed for these genes in *hy5 bbx2021* (Figure 7a-f). Furthermore, *hy5* suppressed the elevated expression of these genes in the *smax1 smxl2* mutant to a similar degree as *bbx2021*. The *smax1 smxl2 hy5 bbx2021* quintuple mutant did not show further inhibition of expression compared to *smax1 smxl2 hy5* and *smax1 smxl2 bbx2021* (Figure 7a-f). These results further support the notion that HY5 and BBX20/21 are functioning together downstream of the KAR signaling pathway to regulate gene expression. Consistently, *hy5* and *hy5 bbx2021* also suppressed the high levels of anthocyanin accumulation in *smax1 smxl2* to similar levels (Figure 7g). This suggests that the HY5-BBX20/21 module promotes anthocyanin accumulation downstream of SMAX1/SMXL2 through transcriptional activation of anthocyanin biosynthesis genes.

By contrast, but similar to that observed in *bbx2021* seedlings, we did not find evidence for transcriptional regulation of *KUF1*, *DLK2*, or *AT3G60290* by HY5 or the HY5-BBX module (Figure S6a-c). Therefore, the HY5-BBX20/BBX21 module is responsible for regulating a subset of the transcriptional responses downstream of SMAX1 and SMXL2.

BBX20 is post-transcriptionally stabilized by KAI2

Our data suggest that a functional HY5-BBX20/BBX21 module is required for accumulation of anthocyanins in response to KAR_2 or in the *smax1 smxl2* mutant. Although the transcriptional promotion of *BBX20* by the KAR signaling pathway is consistent with the observed increase in BBX20 activity, little is known about the post-transcriptional regulation of BBX20 by KAR. To investigate possible effects on BBX20 protein levels, we treated 3-day-old Col-0 and *kai2* seedlings expressing *GFP-BBX20* with 10 µM KAR_2 for 6 h. The *GFP-BBX20* transgene was expressed under the control of a constitutive *35S* promoter to bypass transcriptional regulation of *BBX20* expression by KAR. These experiments revealed a significant KAI2-dependent accumulation of GFP-BBX20 protein in response to KAR_2 treatment (Figure 8a,b). Furthermore, the levels of GFP-BBX20 protein in the absence of KAR treatment were markedly lower in the *kai2* mutant compared to Col-0 (Figure 8a-d). We confirmed that the decreased abundance of GFP-BBX20 in *kai2* is not caused by differential expression of the transgene (Figure S7c). Therefore, KAI2 activity may stabilize BBX20. We observed that treatment with the proteasomal inhibitor MG132 resulted in stabilization of GPF-BBX20 protein in the *kai2*

© 2021 The Authors.

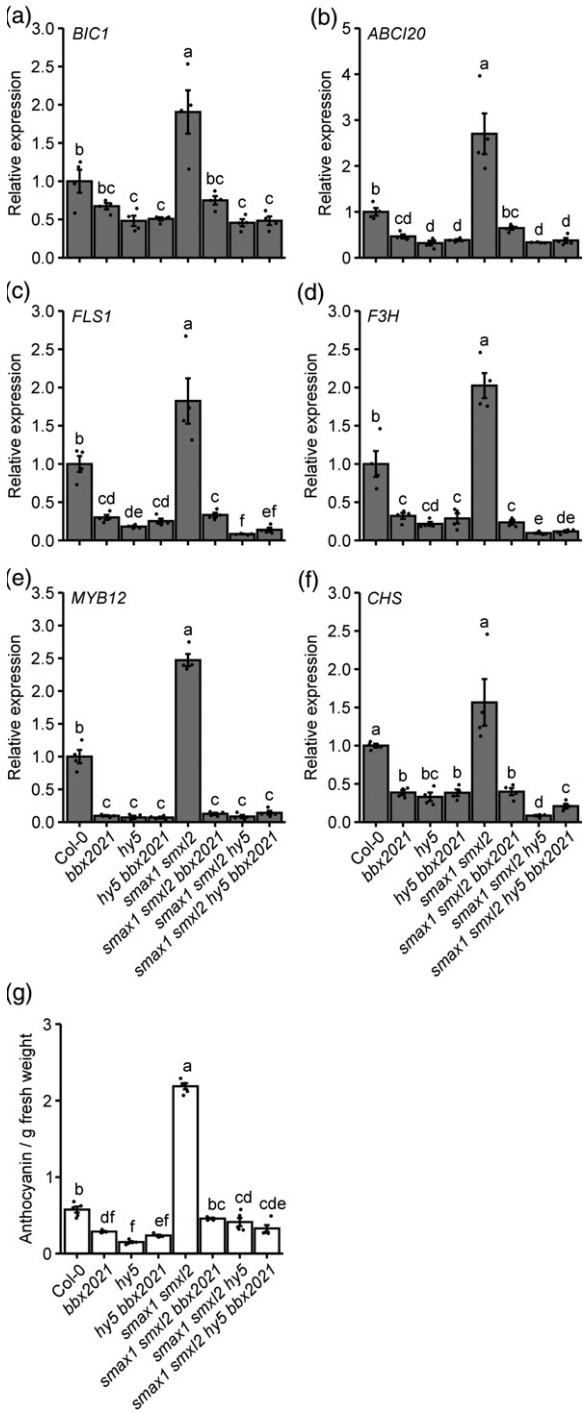

Figure 7. The HY5 – BBX20/BBX21 module promotes anthocyanin biosynthesis downstream of SMAX1 and SMXL2.
(a–f) Transcript abundance of *BIC1* (a), *ABCI20* (b), *FLS1* (c), *F3H* (d), *MYB12* (e), and *CHS* (f) relative to *GADPH* and *TFIID* reference genes in 4-day-old seedlings grown in 80 μmol m^{-2} sec^{-1} red light. (g) Anthocyanin measurements of seedlings grown as in (a) to (f) [$n = 4$ (a–f) and $n = 5$ (g) independent biological replicates are indicated by black dots]. Bars represent the mean and error bars represent the SE and different letters denote statistically significant differences as determined by one-way ANOVA followed by Tukey's *post hoc* test ($P < 0.05$).

mutant, suggesting that BBX20 turnover is mediated by the 26S proteasome (Figure 8e,f).

Following these results, and because we could not detect any transcriptional regulation of BBX21 or HY5 by KAR signaling components (Figure S7a,b), we hypothesized that KAI2 may also affect the stability of BBX21 and HY5. To test this, we crossed lines overexpressing GFP-BBX21 and HY5-GFP with the *kai2* mutant to compare the respective protein levels between the WT and mutant background. Introgression of these transgenes into the *kai2* mutant did not significantly alter their expression (Figure S7d,e). In contrast to GFP-BBX20, *kai2* did not affect GFP-BBX21 or HY5-GFP protein levels (Figure S8a-d).

Overall, these results indicate that KAR/KL signaling mediated by KAI2 promotes the accumulation of BBX20 transcripts and proteins. Both modes of regulation are likely to enhance BBX20 activity.

DISCUSSION

The ability of KARs to promote a variety of light-dependent responses, including germination, inhibition of hypocotyl elongation, cotyledon expansion, anthocyanin accumulation, and chlorophyll accumulation (Nelson *et al.*, 2010; Nelson *et al.*, 2009; Thussagunpanit *et al.*, 2017), makes it abundantly clear that the KAR signaling pathway is closely connected to the light signaling networks. Concordantly, a mutant of *HY5* was found to display severely reduced inhibition of hypocotyl elongation in response to KAR treatment, suggesting a requirement of the HY5 protein for this KAR response (Nelson *et al.*, 2010). However, although the KAR signaling pathway has been reported to elevate *HY5* transcript levels in Arabidopsis seeds (Nelson *et al.*, 2010), regulation of *HY5* levels is unlikely to be the complete mechanism by which KAR promotes HY5 activity because HY5 appears to lack the ability to activate transcription on its own (Oyama *et al.*, 1997; Burko *et al.*, 2020). Several recent studies suggest that BBX20, BBX21, BBX22, and BBX23 act as transcriptional cofactors of HY5 to regulate a subset of HY5 target genes (Bursch *et al.*, 2020; Zhang *et al.*, 2017; An *et al.*, 2019; Bai *et al.*, 2019; Fang *et al.*, 2019). In the present study, we have characterized the role of these BBX proteins in KAR signaling through detailed genetic analysis and found that BBX20, BBX21, and HY5 act together to promote KAR-induced anthocyanin accumulation and inhibition of hypocotyl elongation downstream of SMAX1 and SMXL2.

The HY5-BBX transcriptional module regulates seedling responses to KAR

Because *bbx20* knockout lines were unavailable, the potential role of the BBX20 protein in KAR and SL signaling has previously been analyzed using transgenic lines overexpressing *BBX20* fused with an EAR repression domain

© 2021 The Authors.

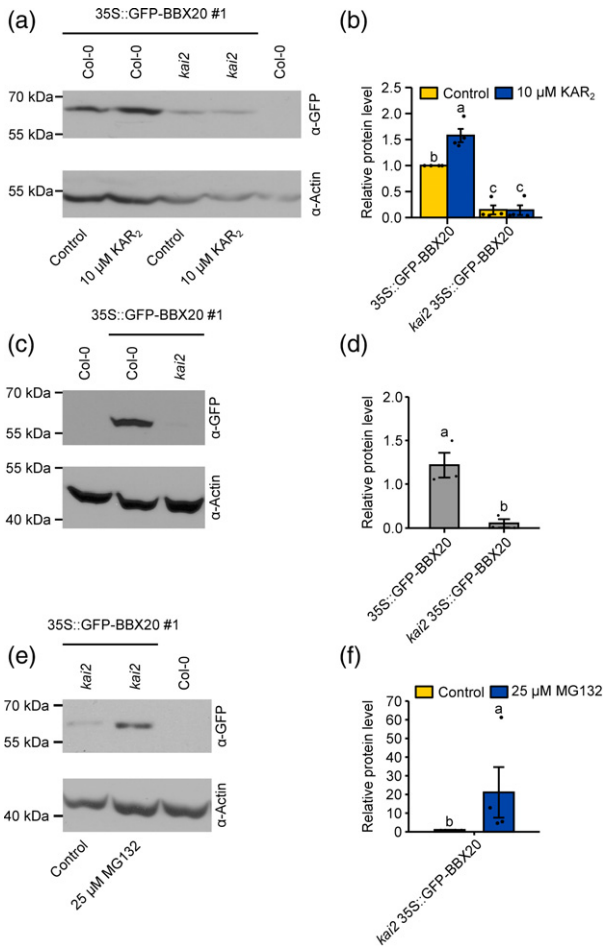

Figure 8. BBX20 accumulates in response to KAR_2 and is destabilized in the *kai2* mutant.

(a, c, e) Immunoblot analysis of total protein samples collected from Col-0 or *kai2* transgenic seedlings expressing GFP-BBX20 grown in 80 μmol m^{-2} sec^{-1} red light. Seedlings were grown for 3 days and treated with 0.1% acetone (control) or 10 μM KAR_2 for 6 h (a), grown for 5 days (c), or grown for 4 days and treated with 0.1% DMSO (control) or 25 μM MG132 for 24 h (e). Anti-GFP and anti-actin antibodies were used to detect the recombinant proteins and the actin loading control, respectively. A representative replicate of three independent biological replicates is shown. (b, d, f) Relative protein levels of BBX20 relative to actin, quantified from the immunoblot analysis in (a), (c) and (e). Bars represent the mean and error bars represent the SE and different letters denote statistically significant differences as determined by a Wilcoxon rank sum test (b) or by a two sample *t*-test (d, f) ($P < 0.05$).

(SRDX) that recruits TPL/TPR proteins (Thussagunpanit *et al.*, 2017; Wei *et al.*, 2016). Although these lines had reduced photomorphogenic development and a reduced response to KAR and *rac*-GR24, the relative contributions of BBX20 and its homologs to these processes may be confounded by the antimorphic nature of the fusion protein. With a CRISPR-Cas9 knockout mutant, we demonstrate that BBX20 indeed plays an important role in KAR-induced inhibition of hypocotyl elongation (Figure 2). Furthermore, we observed that *bbx2021* was largely insensitive to KAR_2 treatment with regards to the inhibition of hypocotyl elongation and induction of anthocyanin accumulation (Figures 3b and 5j). Considering that mutants of *hy5* display a similar insensitivity to KAR treatment (Figure 6a) (Nelson *et al.*, 2010; Waters and Smith, 2013) and that the BBX proteins can act as cofactors for transcriptional regulation by HY5 (Bursch *et al.*, 2020), these results are consistent with KAR signaling acting through the HY5-BBX transcriptional module. This conclusion was also supported by analysis of higher order mutants. First, *hy5* and *bbx2021* fully suppressed the elevated anthocyanin levels of the *smax1 smxl2* mutant, and no additional phenotype was observed in the *smax1 smxl2 hy5 bbx2021* quintuple mutant (Figure 7g). Second, both *hy5* and *bbx2021* were epistatic to *smax1 smxl2* in the regulation of *BIC1*, *ABCI20*, *FLS1*, *F3H*, *MYB12*, and *CHS*, whereas no additional suppression was observed in the quintuple mutant (Figure 7a-f). Overall, these results support a simple pathway in which KAR treatment, or mutation of *SMAX1* and *SMXL2*, partially mimicking the effect of KL, promotes BBX20 and BBX21 activity. In turn, the HY5-BBX20/BBX21 transcriptional module promotes anthocyanin accumulation (Figure 9).

However, the detailed genetic analysis between the *bbx* mutants and *hy5* with the *smax1 smxl2* mutant revealed a more complex pathway when measuring the effects on hypocotyl elongation. First, although *bbx20*, *bbx21*, and *hy5* suppressed the short *smax1 smxl2* hypocotyl phenotype, suggesting increased activity of the HY5-BBX module in the *smax1 smxl2* mutant, this suppression was not complete (Figure 6b). Hence, these results show that SMAX1 and SMXL2 are partially promoting hypocotyl elongation independent of the BBX proteins, HY5, or the HY5-BBX module (Figure 9). Furthermore, because the *hy5* mutant suppressed the *smax1 smxl2* mutant phenotype more strongly than *bbx2021* or *bbx20212223* (Figure 6c), HY5 also appears to have functions independent of the BBX proteins in the context of KAR signaling (Figure 9). We have previously seen that BBX20, BBX21, and BBX22, in their role as transcriptional cofactors of HY5, only account for approximately 15% of HY5-regulated genes (Bursch *et al.*, 2020). Hence, the BBX-independent function of HY5 in regulating hypocotyl elongation downstream of SMAX1 and SMXL2 could indicate the presence of unknown partners to HY5 acting in the KAR signaling pathway (Figure 9). Furthermore, although the *bbx2021* mutant, similar to *hy5*, showed a strongly reduced response to KAR_2 treatment (Figure 3b and Figure S3), little evidence for a genetic interaction was observed when analyzing the *bbx2021 kai2* or *bbx2021 max2* mutants (Figure S4). It has also been concluded that HY5 works largely in a parallel pathway to KAI2 and MAX2 to inhibit hypocotyl elongation (Waters and Smith, 2013). Hence, these observations highlight the fact that the core KAR signaling pathway, consisting of

© 2021 The Authors.

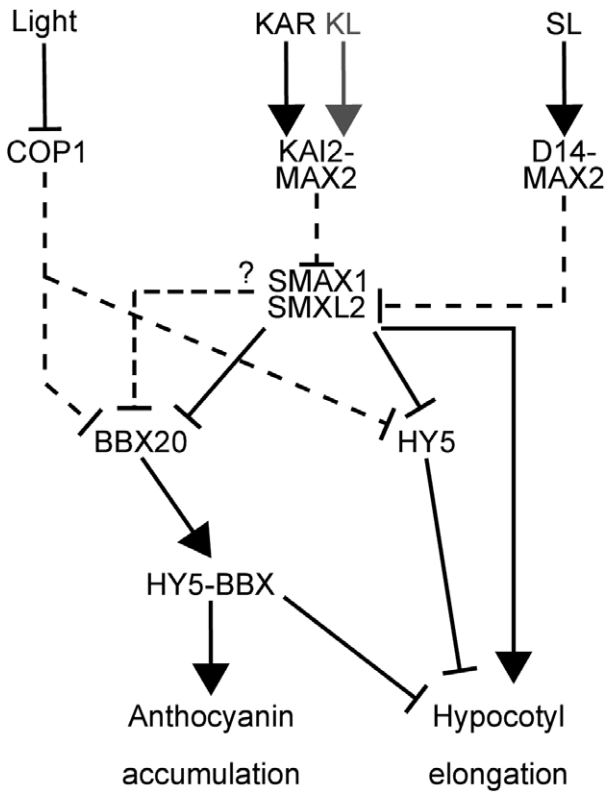

Figure 9. Model of SMAX1- and SMXL2-dependent regulation of photomorphogenesis.
Karrikin (KAR) or a putative KAI2 ligand (KL) promotes the interaction of KAI2 and MAX2, which act as a complex targeting SMAX1 and SMXL2 for degradation. Similarly, application of strigolactone (SL) promotes the formation of a D14-MAX2 complex, which targets SMXL2. BBX20 and HY5 accumulate in response to light-dependent inactivation of COP1, whereas *BBX20* is transcriptionally suppressed by SMAX1 and SMXL2. BBX20 is also post-transcriptionally stabilized by KAR, dependent on KAI2 and most likely SMAX1 and SMXL2. HY5 and the BBX proteins act as a transcriptional module promoting gene expression resulting in increased accumulation of anthocyanins. Hence, light- and SMAX1/SMXL2-dependent signaling intersect on HY5 and the BBX proteins. However, HY5 partially inhibits hypocotyl elongation downstream of SMAX1 and SMXL2 independently of the BBX proteins, and SMAX1 and SMXL2 can partially promote elongation independently of HY5. Dashed lines indicate post-transcriptional regulation.

KAI2, MAX2, SMAX1, and SMXL2, has functions independent of the HY5-BBX module and suggest that removal of KAI2 or MAX2 might specifically promote the HY5-BBX independent pathway by which SMAX1 and SMXL2 promote hypocotyl elongation (Figure 9).

By contrast to *kai2*, neither SL-insensitive *d14*, nor SL-deficient *max* mutants show defects in the inhibition of hypocotyl elongation (Nelson *et al.*, 2011; Scaffidi *et al.*, 2013). However, application of exogenous SL or GR24 inhibits hypocotyl elongation. This response is mediated by D14-dependent destabilization of SMXL2 (Wang *et al.*, 2020). Hence, our genetic analysis of higher order mutants using *smax1 smxl2* might also be applicable to the effects of exogenously added SLs on photomorphogenic development (Figure 9). This notion is supported by the fact that both HY5 and BBX20 have been implicated in GR24-dependent inhibition of hypocotyl elongation (Jia *et al.*, 2014; Wei *et al.*, 2016).

Transcriptional regulation downstream of SMAX1 and SMXL2

The comparison of transcriptomic changes between *bbx2021* and *smax1 smxl2* revealed a subset of genes that are regulated by SMAX1 and SMXL2 through the HY5-BBX transcriptional module. However, most misregulated genes in *smax1 smxl2* do not depend on HY5-BBX (Figures 5 and S5). Interestingly the list of DEGs in the *smax1 smxl2* mutant was enriched for genes involved in photosynthesis and translation. These results are in line with the early proteome responses observed in Arabidopsis seedlings after short-term KAR treatment (Baldrianová *et al.*, 2015). Furthermore, because our transcriptomic analysis of the *smax1 smxl2* mutant represented the first analysis of a constitutive KAR signaling mutant, we further compared our dataset with previously published transcriptome datasets for the KAR-insensitive *kai2* and *max2* mutants. Despite the very distinct experimental conditions, we were able to identify a list of high-confidence KAR target genes that are oppositely regulated in *kai2* and *max2* versus *smax1 smxl2* (Figure S5). Reassuringly, this list contained the often-used marker genes *KUF1*, *DLK2*, and *BBX20*, which have homologs in *Brassica tournefortii* that are also strongly promoted by KAR treatment (Sun *et al.*, 2020). The suggestion that SMAX1 and SMXL2 function in a transcriptional repressor complex (Soundappan *et al.*, 2015) led us to the hypothesis that these genes, amongst the other genes from this list upregulated in *smax1 smxl2*, might represent a core set of possible direct targets of SMAX1 and SMXL2.

Interestingly the list of high-confidence KAR response genes contains a number of auxin-responsive genes that are downregulated in *smax1 smxl2* but upregulated in *kai2* and *max2* (Figure S5C). Treatment of the *max2* mutant with the auxin transport inhibitor NPA suggested that enhanced auxin transport contributes to the elongated hypocotyl phenotype of *max2* (Shen *et al.*, 2012). Similarly, the *kai2* mutant phenotypes were recently shown to be suppressed by both NPA and the auxin efflux carrier triple mutant *pin3 pin4 pin7*. Consistently, KAI2 was shown to modulate the abundance of several PIN proteins, likely contributing to the *kai2* phenotype (Hamon-Josse *et al.*, 2021). Although the effect of SMAX1 and SMXL2 on auxin transport is less clear, the SL pathway targets SMXL6, SMXL7, and SMXL8 promote auxin transport, likely by promoting accumulation of PIN1 at the basal plasma membrane (Soundappan *et al.*, 2015). Hence, the downregulation of the auxin response genes in *smax1*

© 2021 The Authors.
The Plant Journal published by Society for Experimental Biology and John Wiley & Sons Ltd.,

smxl2 may be a consequence of altered auxin transport, which might also contribute to the shortened hypocotyl phenotype of *smax1 smxl2*.

The HY5-BBX module as a point of convergence of light and KAR/SL signaling

As targets of COP1/SPA-dependent degradation, HY5 and the BBX proteins accumulate in response to light but not in darkness (Fan *et al.*, 2012; Osterlund *et al.*, 2000; Xu *et al.*, 2016). Hence, the reported inability of KAR to modulate hypocotyl elongation in etiolated Arabidopsis seedlings (Nelson *et al.*, 2010) is consistent with a lack of the HY5-BBX module components in these conditions. Similarly, photoreceptor mutants have been shown to be hyposensitive to KAR and *rac*-GR24 when grown in light (Jia *et al.*, 2014; Nelson *et al.*, 2010), whereas mutants of *COP1* show hypocotyl elongation responses to KAR and *rac*-GR24 when grown in darkness (Jia *et al.*, 2014; Lee *et al.*, 2019). These observations are all consistent with KAR signaling requiring an activated light signaling pathway, including COP1 inactivation and accumulation of HY5 and the BBX proteins, to generate a robust developmental response in seedlings. Interestingly, high levels of *rac*-GR24 have been shown to promote de-etiolation in dark-grown seedlings. This response was attributed to reduced nuclear levels of COP1 resulting in increased HY5 accumulation in darkness (Toh *et al.*, 2014). However, under high levels of *rac*-GR24, inhibition of hypocotyl elongation in darkness is largely independent of MAX2 or SMAX1 and SMXL2 (Jia *et al.*, 2014; Stanga *et al.*, 2016; Tsuchiya *et al.*, 2010). By contrast, HY5 was also shown to undergo COP1-independent accumulation in response to more moderate levels of 10 μM *rac*-GR24, dependent on MAX2, suggesting a separate pathway for HY5 stabilization (Tsuchiya *et al.*, 2010). Similarly, BBX20 has been shown to accumulate in response to moderate levels of *rac*-GR24, which might be dependent on either D14 or KAI2 activation by *rac*-GR24 (Wei *et al.*, 2016). In line with these observations, we observed accumulation of BBX20 in response to KAR_2 and destabilization of BBX20 in the *kai2* background, suggesting that the activity of the HY5-BBX module is regulated at the transcriptional and post-transcriptional levels (Figure 8a-d).

By contrast to the studies showing *rac*-GR24-dependent accumulation of HY5, we did not observe any influence of *kai2* on HY5 protein levels (Figure 8e). However, promotion of photomorphogenesis by the HY5-BBX module is mainly dependent on the rate-limiting, transactivation domain-containing BBX proteins, whereas overexpression of HY5 has little effect (Bursch *et al.*, 2020; Ang *et al.*, 1998; Burko *et al.*, 2020). Consequently, although the *hy5* mutant lacks a functional HY5-BBX transcriptional module, KAI2-dependent stabilization of HY5 would not be expected to strongly contribute to the observed phenotypes. Nevertheless, in contrast to BBX20, we did not observe any regulation of BBX21 by KAR signaling at the transcriptional or post-transcriptional level (Figures 8d and S8). On the one hand, this can suggest that regulation of BBX21 is not necessary because HY5, BBX20, and BBX21 could work in a protein complex for which the regulation of one component is already sufficient to enhance the complex activity. On the other hand, our genetic analysis clearly shows that *bbx20* has a greater impact on the *smax1 smxl2* phenotype than *bbx21* (Figure 4b), compatible with the less-pronounced regulation of BBX21 by the KAR pathway.

In summary, our data suggest that light and KAR signaling intersect at the HY5-BBX module to promote accumulation of anthocyanins and partially inhibit hypocotyl elongation in response to KAR/KL. BBX20 activity is positively regulated by KAI2-dependent signaling through transcriptional upregulation and increased protein stability. BBX20 acts together with BBX21 and HY5 to control the expression of a subset of SMAX1- and SMXL2-regulated genes.

EXPERIMENTAL PROCEDURES

Plant material and growth conditions

The *bbx20-1*, *bbx21-1*, *bbx22-1*, *bbx23-1*, *hy5-215*, *hyh*, *kai2* (*htl-3*), *max2-1*, and *smax1-2 smxl2-1* mutants originate from Arabidopsis Col-0 accession and have been described previously (Bursch *et al.*, 2020; Datta *et al.*, 2008; Datta *et al.*, 2007; Oyama *et al.*, 1997; Sentandreu *et al.*, 2011; Stanga *et al.*, 2016; Stirnberg *et al.*, 2002; Toh *et al.*, 2014; Zoulias *et al.*, 2020). The *bbx21-2* (GT_5_101627) mutant originates from Arabidopsis Ler accession and was described previously (Datta *et al.*, 2007). The *bbx20-2* was created using CRISPR-Cas9, as described previously for *bbx20-1* (Bursch *et al.*, 2020), but in the L*er* background and was backcrossed to the WT background two times. Removal of the CRISPR-Cas9 cassette was confirmed by PCR. All higher order mutants were obtained by genetic crossing and subsequent PCR-based genotyping or by phenotype in the case of *max2-1*. The primers used for genotyping are listed in Table S3. 35S::GFP-BBX20 #1 and 35S::GFP-BBX21 #2 were described previously (Bursch *et al.*, 2020). To create 35S::HY5-GFP, the coding sequence of *HY5* lacking the stop codon was shuttled from pDONR221-HY5_ns (Bursch *et al.*, 2020) via Gateway LR reaction into pK7FWG2 (Karimi *et al.*, 2002) and transformed into *hy5-215* via the *Agrobacterium* floral dip method. To create the pBBX20::GUS-GFP transgenic lines, a 2-kb fragment of the *BBX20* promoter was amplified with the primers pBBX20_F and pBBX20_R and shuttled into pDONR221 via Gateway BP reaction. The fragment was subsequently shuttled via Gateway LR reaction into pKGWFS7 (Karimi *et al.*, 2002) and transformed into Arabidopsis Col-0 via the floral dip method. The primers used for cloning are listed in Table S3. Two independent transgenic lines were then crossed with the *smax1 smxl2* mutant.

Seeds were surface-sterilized and sown on ½ MS medium [0.05% (w/v) MES, pH 5.7, 1% (w/v) agar]. To analyze the effect of KAR_2 treatment, the medium was supplemented with 0.1% (v/v) acetone (control) or various concentrations of KAR_2 as indicated. Seeds were stratified for 2–3 days at 4°C in darkness, followed by 4 or 5 days of growth in red light (70 μmol m^{-2} sec^{-1}).

© 2021 The Authors.

Phenotypic analysis

For hypocotyl measurements, 5-day-old seedlings were flattened on the growth medium and photographed before measurements were performed using IMAGEJ (https://imagej.nih.gov/ij).

For anthocyanin measurements, 4-day-old seedlings grown on ½ MS medium with sucrose [0.05% (w/v) MES, pH 5.7, 1% (w/v) sucrose, 1% (w/v) agar] were harvested, weighed, and flash-frozen in liquid nitrogen. After grinding the frozen material to a powder, 600 μl of anthocyanin extraction buffer (1% (v/v) HCl in methanol) was added and the samples were incubated in darkness at 4°C overnight. Then, 650 μl of chloroform and 200 μl of H_2O were added to each sample and vortexed before being centrifuged for 10 min at 16 000 ***g***. Anthocyanin levels were estimated by spectrophotometric measurement of the absorbance (*A*) of the upper liquid phase (A_{530} and A_{657}) and calculated using: $(A_{530} - 0.33 \times A_{657})$/[tissue weight (g)].

All phenotypic analyses were performed three times with similar results.

Germination assay

To determine germination rates, approximately 100 seeds per biological replicate were sown on ½ MS medium containing 0.1% acetone or 1 μM KAR_2. The seeds were stratified for 3 days at 4°C and germination was counted 24, 48 and 72 h after incubation in constant red light (approximately 80 μmol m^{-2} sec^{-1}).

Analysis of transcript levels

For total RNA isolation, samples were stratified for 2–3 days at 4°C before incubation in red light (approximately 80 μmol m^{-2} sec^{-1}) for 4 days. The seedlings were then harvested and frozen in liquid nitrogen. Four biological replicates were analyzed for each genotype. To analyze tissue-specific transcriptional changes in response to KAR treatment, the seedlings were harvested in RNA*later* solution (Thermo Scientific, Waltham, MA, USA) prior to the dissection of cotyledons and hypocotyls followed by RNA extraction.

Total RNA was extracted using RNeasy Plant Mini Kit (Qiagen, Valencia, CA, USA) in accordance with the manufacturer's instructions, including on-column DNAse treatment. A two-step qRT-PCR analysis was performed. First, cDNA was synthesized using Superscript III Reverse Transcriptase (Invitrogen, Carlsbad, CA, USA) with random N9 and dT_{25} primers in accordance with the manufacturer's instructions. The primer pairs used for qPCR reactions on cDNA templates are listed in Table S3. The qPCR was performed using the CFX96 Real-Time System (Bio-Rad, Hercules, CA, USA). *GADPH* and *TFIID* or *UBC21* and *PP2A* were used as reference genes as indicated and transcript levels relative to the controls were calculated as described previously (Vandesompele *et al.*, 2002).

For RNA-seq, total RNA was extracted from Col-0, *bbx2021* and *smax1 smxl2* seedlings that were grown as described above. RNA was extracted as described previously (Sokolovsky *et al.*, 1990). In brief, samples were flash-frozen in liquid nitrogen and ground to a powder. The powder was dissolved in 750 μl of extraction buffer [0.6 M NaCl, 10 mM EDTA, 4% (w/v) SDS, 0.1 M Tris-HCl, pH 7.5] and 750 μl of phenol/chloroform/isoamyl alcohol solution (25:24:1). After shaking the samples for 10 min, they were centrifuged at 16 000 ***g*** for 5 min. The supernatant was mixed 1:1 with chloroform/isoamyl alcohol (24:1) solution. After centrifugation for 3 min at maximum speed, the supernatant was mixed with 340 μl of 8 M LiCl. After incubation on ice for 30 min followed by centrifugation of 15 min at 4°C, the pellet was dissolved in RNase-free water, mixed with 30 μl of 3 M sodium acetate, pH 5.2, and 700 μl of absolute ethanol. After incubation at −80°C for 30 min and centrifugation, the pellet was washed with 70% ethanol (v/v) and the RNA was dissolved in RNase-free water. RNA was cleaned up and on-column DNAse treatment was performed with the RNeasy Plant Mini Kit (Qiagen) in accordance with the manufacturer's instructions. Three independent biological replicates were sent to BGI (Hong Kong, China) for RNA quality and integrity control, library synthesis, high-throughput sequencing, and bioinformatic analysis. In short, an Model 2100 Bioanalyzer (Agilent, Santa Clara, CA, USA) was used to measure RNA concentration, RIN value, 28S/18S, and fragment length distribution. A NanoDrop™ spectrophotometer (Thermo Fisher) was used to identify the purity of RNA samples. The mRNA was enriched by using oligo (dT) magnetic beads and double-stranded cDNA was synthesized with random hexamer primers. After end-repair the cDNA was 3′ adenylated and adaptors were ligated to the adenylated cDNA. The ligation products were purified and enriched via PCR amplification, followed by denaturation and cyclization. The library products were sequenced via the BGISEQ-500 platform. The raw sequencing reads (> 26 million per sample) were filtered by removing reads with adaptors, reads with unknown bases, and low quality reads. Clean reads (approximately 26 million per sample) were stored in FASTQ format (Cock *et al.*, 2010). The clean reads were mapped to TAIR10 using Bowtie2 (Langmead and Salzberg, 2012) and gene expression level was calculated with RSEM (Li and Dewey, 2011). Differentially expressed genes were identified with the Deseq2 (Love *et al.*, 2014) method with the following criteria: fold-change ≥ 1.5 and Bonferroni adjusted $P \leq 0.05$.

GO-term analysis

GO-term analysis was performed with the 'PANTHER Overrepresentation Test' using the GO Ontology (https://doi.org/10.5281/zenodo.4081749, released 2020-10-09) as described previously (Mi *et al.*, 2019) utilizing the 'GO biological process complete' annotation data set.

GUS staining

For GUS staining, seeds were sown on ½ MS containing 0.1% acetone (v/v) (control) or 1 μM KAR_2, stratified for 2 days, and then incubated in red light (approximately 80 μmol m^{-2} sec^{-1}) for 24, 48, or 96 h. The GUS staining (Hemerly *et al.*, 1993) and subsequent clearing (Malamy and Benfey, 1997) was performed as described previously. After the harvest, seedlings were incubated in 90% acetone at −20°C for 1 h. The samples were washed twice with a 50 mM sodium phosphate buffer (pH 7.0) and then incubated in the staining solution [10 mM potassium ferricyanide, 10 mM potassium ferrocyanide, 1 mM 5-bromo-4-chloro-3-indolyl β-D-glucuronic acid, 0.2% (v/v) Triton X-100 in 50 mM sodium phosphate buffer (pH 7.0)] at 37°C overnight. To clear the tissue, seedlings were incubated in a solution of 0.24 M HCl in 20% ethanol at 57°C for 15 min. The solution was replaced with a solution of 7% NaOH (w/v) in 60% Ethanol and the samples were incubated for 15 min at room temperature. After stepwise rehydration in 40%, 20%, and 10% ethanol, the samples were incubated in a solution of 25% glycerine in 5% ethanol for 15 min at room temperature. Pictures were taken with a stereomicroscope (SZX12; Olympus, Shinjuku, Japan) or a microscope (Axioskop 2 plus; Zeiss, Jena, Germany) equipped with an Olympus C-4040ZOOM camera.

© 2021 The Authors.

Immunoblotting

For analyzing protein levels in response to KAR_2, seedlings were grown in red light (80 μmol m^{-2} sec^{-1}) for 3 days before treatment with liquid ½ MS supplemented with 0.1% acetone (control) or 10 μM KAR_2 for 6 h before harvest. For MG132 experiments, 4-day-old seedlings were incubated with liquid ½ MS supplemented 0.1% DMSO (control) or 25 μM MG132 for 24 h and harvested on day 5. Seedlings without treatment were grown for 5 days. After harvest, seedlings were flash-frozen in liquid nitrogen and ground to a fine powder using a tissue lyser. Extraction buffer [50 mM Tris-HCl pH 7.5, 150 mM NaCl, 1% (w/v) sodium deoxycholate, 0.5% Triton X-100, 1 mM DTT, 50 μM MG132, 50 μM MG115, 1 × COMPLETE protease inhibitor cocktail (EDTA-free; Roche, Basel, Switzerland)] was added and the samples were centrifuged for 10 min at 16 000 ***g*** and 4°C. The total protein sample, collected from the supernatant, was then separated on a 10% SDS-PAGE and transferred to a polyvinylidene fluoride membrane. After blocking with 6% (w/v) skim milk powder in PBS-T, anti-GFP (#632380; Takara Bio Clontech, Shiga, Japan) and anti-ACT (#A0480; Sigma, St Louis, MO, USA) were used at dilutions of 1:2000 and 1:10 000, respectively, followed by the secondary anti-mouse-horseradish peroxidase (#31431; Thermo Scientific) at a dilution of 1:10 000 in blocking solution. For protein detection, the membrane was incubated with SuperSignal West Pico Chemiluminescent Substrate (Thermo Scientific) in accordance with the manufacturer's instructions using CL-Xposure Films (Thermo Scientific). Quantification of the immunoblots was performed using IMAGEJ (https://imagej.nih.gov/ij).

Statistical analysis

Statistical analysis was performed with R studio, version 1.2.1335 (http://www.rstudio.com). The data was tested for equal variances using Brown–Forsythe test (car package version 3.0-6) and for normal distribution by the Shapiro–Wilk test. Log transformed or non-transformed data were then analysed by one-way or two-way ANOVA followed by Tukey's *post hoc* test or the Wilcoxon rank sum test (stats package version 4.0.2). Statistically significant differences ($P < 0.05$) are indicated by different letters. Boxplots were generated with ggplot2 (version 3.2.1), where outliers are defined as greater than the 1.5 × interquartile range.

ACKNOWLEDGEMENTS

We thank Cordula Braatz for technical assistance. This project was funded by the Deutsche Forschungsgemeinschaft (DFG, German Research Foundation) – Project numbers 409212330; 320656366 to HJ and by National Science Foundation IOS-1856741 to DCN. Open Access funding enabled and organized by Projekt DEAL.

CONFLICT OF INTEREST

The authors declare no conflict of interest.

AUTHOR CONTRIBUTIONS

HJ and KB designed the research with input from DCN. KB performed all the experiments. KB and HJ analyzed the data. ETN generated *bbx20-2* and higher order mutants and performed preliminary experiments. HJ, KB and DCN wrote the manuscript.

DATA AVAILABILITY STATEMENT

The RNA-seq data have been deposited in the NCBI Gene Expression Omnibus (GSE166857).

SUPPORTING INFORMATION

Additional Supporting Information may be found in the online version of this article.

Figure S1. *BBX20* promoter activity of a second transgenic line.

Figure S2. KAR_2 response curves in *bbx20* mutants.

Figure S3. Analysis of the KAR response of *bbx20* and *bbx21* mutants from the L*er* ecotype.

Figure S4. Genetic interaction of *bbx2021* and *kai2* and *max2*.

Figure S5. Analysis of SMAX1 and SMXL2 regulated genes.

Figure S6. Transcriptional regulation of *KUF1*, *DLK2*, and *AT3G60290* in *smax1 smxl2 hy5 bbx2021*.

Figure S7. Analysis of BBX21 and HY5 protein levels in the *kai2* mutant.

Figure S8. *BBX21* and *HY5* transcript levels in KAR signaling mutants.

Table S1. Comparison of DEGs of *bbx2021* and *smax1 smxl2* with *HY5*-regulated genes.

Table S2. Comparison of DEGs of *smax1 smxl2* with *KAI2*- and *MAX2*-regulated genes.

Table S3. Primers used in the present study.

Data S1. DEGs of *bbx2021* and *smax1 smxl2*.

REFERENCES

An, J.-P., Wang, X.-F., Zhang, X.-W., Bi, S.-Q., You, C.-X. & Hao, Y.-J. (2019) MdBBX22 regulates UV-B-induced anthocyanin biosynthesis through regulating the function of MdHY5 and is targeted by MdBT2 for 26S proteasome-mediated degradation. *Plant Biotechnology Journal*, **17**, 2231–2233.

Ang, L.H., Chattopadhyay, S., Wei, N., Oyama, T., Okada, K., Batschauer, A. *et al.* (1998) Molecular interaction between COP1 and HY5 defines a regulatory switch for light control of Arabidopsis development. *Molecular Cell*, **1**, 213–222.

Bai, S., Tao, R., Yin, L., Ni, J., Yang, Q., Yan, X. *et al.* (2019) Two B-box proteins, PpBBX18 and PpBBX21, antagonistically regulate anthocyanin biosynthesis via competitive association with Pyrus pyrifolia ELONGATED HYPOCOTYL 5 in the peel of pear fruit. *The Plant Journal*, **100**, 1208–1223. https://doi.org/10.1111/tpj.14510.

Baldrianová, J., Černý, M., Novák, J., Jedelský, P.L., Divíšková, E. & Brzobohatý, B. (2015) Arabidopsis proteome responses to the smoke-derived growth regulator karrikin. *Journal of Proteomics*, **120**, 7–20.

Bennett, T. & Leyser, O. (2014) Strigolactone signalling: standing on the shoulders of DWARFs. *Current Opinion in Plant Biology*, **22**, 7–13.

Blázquez, M.A., Nelson, D.C. & Weijers, D. (2020) Evolution of plant hormone response pathways. *Annual Review of Plant Biology*, **71**(1), 327–353. https://doi.org/10.1146/annurev-arplant-050718-100309.

Burko, Y., Seluzicki, A., Zander, M., Pedmale, U.V., Ecker, J.R. & Chory, J. (2020) Chimeric activators and repressors define HY5 activity and reveal a light-regulated feedback mechanism. *The Plant Cell*, **32**(4), 967–983. https://doi.org/10.1105/tpc.19.00772.

Bursch, K., Toledo-Ortiz, G., Pireyre, M., Lohr, M., Braatz, C. & Johansson, H. (2020) Identification of BBX proteins as rate-limiting cofactors of HY5. *Nature Plants*, **6**(8), 921–928. https://doi.org/10.1038/s41477-020-0725-0.

Bythell-Douglas, R., Rothfels, C.J., Stevenson, D.W.D., Graham, S.W., Wong, G.-K.-S., Nelson, D.C. *et al.* (2017) Evolution of strigolactone receptors by gradual neo-functionalization of KAI2 paralogues. *BMC Biology*, **15**, 52.

Chang, C.-S.-J., Li, Y.-H., Chen, L.-T. Chen, W-C, Hsieh, W-P, Shin, J, *et al.* (2008) LZF1, a HY5-regulated transcriptional factor, functions in Arabidopsis de-etiolation. *The Plant Journal*, **54**(2), 205–219.

Chang, C.-S.-J., Maloof, J.N. & Wu, S.-H. (2011) COP1-mediated degradation of BBX22/LZF1 optimizes seedling development in Arabidopsis. *Plant Physiology*, **156**, 228–239.

Choi, J., Lee, T., Cho, J., Servante, E. K., Pucker, B., Summers, W. *et al.* (2020) The negative regulator SMAX1 controls mycorrhizal symbiosis and strigolactone biosynthesis in rice. *Nature Communications*, **11**, 2114.

© 2021 The Authors.

Cock, P.J.A., Fields, C.J., Goto, N., Heuer, M.L. & Rice, P.M. (2010) The Sanger FASTQ file format for sequences with quality scores, and the Solexa/Illumina FASTQ variants. *Nucleic Acids Research*, **38**, 1767–1771.

Conn, C.E. & Nelson, D.C. (2015) Evidence that KARRIKIN-INSENSITIVE2 (KAI2) Receptors may Perceive an Unknown Signal that is not Karrikin or Strigolactone. *Frontiers in Plant Science*, **6**, 1219.

Datta, S., Hettiarachchi, C., Johansson, H. & Holm, M. (2007) SALT TOLERANCE HOMOLOG2, a B-box protein in Arabidopsis that activates transcription and positively regulates light-mediated development. *The Plant Cell*, **19**, 3242–3255.

Datta, S., Johansson, H., Hettiarachchi, C., Irigoyen, M.L., Desai, M., Rubio, V. *et al.* (2008) LZF1/SALT TOLERANCE HOMOLOG3, an Arabidopsis B-box protein involved in light-dependent development and gene expression, undergoes COP1-mediated ubiquitination. *The Plant Cell*, **20**, 2324–2338.

Dixon, K.W., Merritt, D.J., Flematti, G.R. & Ghisalberti, E.L. (2009) Karrikinolide–a phytoreactive compound derived from smoke with applications in horticulture, ecological restoration and agriculture. *Acta Horticulture*, **813**, 155–170.

Fan, X.-Y., Sun, Y., Cao, D.-M., Bai, M.-Y., Luo, X.-M., Yang, H.-J. *et al.* (2012) BZS1, a B-box protein, promotes photomorphogenesis downstream of both brassinosteroid and light signaling pathways. *Molecular Plant*, **5**, 591–600.

Fang, H., Dong, Y., Yue, X., Hu, J., Jiang, S., Xu, H. *et al.* (2019) The B-box zinc finger protein MdBBX20 integrates anthocyanin accumulation in response to ultraviolet radiation and low temperature. *Plant, Cell and Environment*, **42**, 2090–2104.

Flematti, G.R., Ghisalberti, E.L., Dixon, K.W. & Trengove, R.D. (2004) A compound from smoke that promotes seed germination. *Science*, **305**, 977.

Flematti, G.R., Ghisalberti, E.L., Dixon, K.W. & Trengove, R.D. (2009) Identification of alkyl substituted 2H-Furo[2,3-c]pyran-2-ones as germination stimulants present in smoke. *Journal of Agriculture and Food Chemistry*, **57**, 9475–9480.

Gomez-Roldan, V., Fermas, S., Brewer, P.B., Puech-Pagès, V., Dun, E.A., Pillot, J.-P. *et al.* (2008) Strigolactone inhibition of shoot branching. *Nature*, **455**, 189–194.

Guo, Y., Zheng, Z., La Clair, J.J., Chory, J. & Noel, J.P. (2013) Smoke-derived karrikin perception by the α/β-hydrolase KAI2 from Arabidopsis. *Proceedings of the National Academy of Sciences of the United States of America*, **110**, 8284–8289.

Gutjahr, C., Gobbato, E., Choi, J., Riemann, M., Johnston, M.g., Summers, W. *et al.* (2015) Rice perception of symbiotic arbuscular mycorrhizal fungi requires the karrikin receptor complex. *Science*, **350**, 1521–1524.

Hamon-Josse, M., Villaecija-Aguilar, J.A., Ljung, K., Leyser, O., Gutjahr, C. & Bennett, T. (2021) KAI2 regulates seedling development by mediating light-induced remodelling of auxin transport. *BioRxiv*, p. 2021.05.06.443001.

Hemerly, A.S., Ferreira, P., de Almeida Engler, J., Van Montagu, M., Engler, G. & Inzé, D. (1993) cdc2a expression in Arabidopsis is linked with competence for cell division. *The Plant Cell*, **5**, 1711–1723.

Holm, M., Ma, L.-G., Qu, L.-J. & Deng, X.-W. (2002) Two interacting bZIP proteins are direct targets of COP1-mediated control of light-dependent gene expression in Arabidopsis. *Genes & Development*, **16**, 1247–1259.

Hrdlička, J., Gucký, T., Novák, O., Kulkarni, M., Gupta, S., van Staden, J. *et al.* (2019) Quantification of karrikins in smoke water using ultra-high performance liquid chromatography–tandem mass spectrometry. *Plant Methods*, **15**, 81.

Jia, K.-P., Luo, Q., He, S.-B., Lu, X.-D. & Yang, H.-Q. (2014) Strigolactone-regulated hypocotyl elongation is dependent on cryptochrome and phytochrome signaling pathways in Arabidopsis. *Molecular Plant*, **7**, 528–540.

Jiang, L., Liu, X., Xiong, G., Liu, H., Chen, F., Wang, L. *et al.* (2013) DWARF 53 acts as a repressor of strigolactone signalling in rice. *Nature*, **504**, 401–405.

Karimi, M., Inzé, D. & Depicker, A. (2002) GATEWAY™ vectors for Agrobacterium-mediated plant transformation. *Trends in Plant Science*, **7**, 193–195.

Khanna, R., Kronmiller, B., Maszle, D.R., Coupland, G., Holm, M., Mizuno, T. *et al.* (2009) The Arabidopsis B-box zinc finger family. *The Plant Cell*, **21**, 3416–3420.

Khosla, A., Morffy, N., Li, Q., Faure, L., Chang, S. H., Yao, J. *et al.* (2020) Structure–Function Analysis of SMAX1 Reveals Domains That Mediate Its Karrikin-Induced Proteolysis and Interaction with the Receptor KAI2. *The Plant Cell*, **32**(8), 2639–2659. https://doi.org/10.1105/tpc.19.00752.

Langmead, B. & Salzberg, S.L. (2012) Fast gapped-read alignment with Bowtie 2. *Nature Methods*, **9**, 357–359.

Lee, I., Choi, S., Lee, S. & Soh, M.-S. (2019) KAI2-KL signaling intersects with light-signaling for photomorphogenesis. *Plant Signaling & Behavior*, **14**, e1588660.

Li, B. & Dewey, C.N. (2011) RSEM: accurate transcript quantification from RNA-Seq data with or without a reference genome. *BMC Bioinformatics*, **12**, 323.

Li, W., Nguyen, K.H., Chu, H.D., Ha, C.V., Watanabe, Y., Osakabe, Y. *et al.* (2017) The karrikin receptor KAI2 promotes drought resistance in Arabidopsis thaliana. *PLoS Genetics*, **13**, e1007076.

Love, M.I., Huber, W. & Anders, S. (2014) Moderated estimation of fold change and dispersion for RNA-seq data with DESeq2. *Genome Biology*, **15**, 550.

Malamy, J.E. & Benfey, P.N. (1997) Organization and cell differentiation in lateral roots of Arabidopsis thaliana. *Development*, **124**, 33–44.

Merritt, D.J., Kristiansen, M., Flematti, G.R., Turner, S.R., Ghisalberti, E.L., Trengove, R.D. *et al.* (2006) Effects of a butenolide present in smoke on light-mediated germination of Australian Asteraceae. *Seed Science Research*, **16**, 29–35.

Mi, H., Muruganujan, A., Huang, X., Ebert, D., Mills, C., Guo, X. & Thomas, P.D. (2019) Protocol Update for large-scale genome and gene function analysis with the PANTHER classification system (v.14.0). *Nature Protocols*, **14**(3), 703–721.

Nelson, D.C., Flematti, G.R., Ghisalberti, E.L., Dixon, K.W. & Smith, S.M. (2012) Regulation of seed germination and seedling growth by chemical signals from burning vegetation. *Annual Review of Plant Biology*, **63**, 107–130.

Nelson, D.C., Flematti, G.R., Riseborough, J.-A., Ghisalberti, E.L., Dixon, K.W. & Smith, S.M. (2010) Karrikins enhance light responses during germination and seedling development in Arabidopsis thaliana. *Proceedings of the National Academy of Sciences of the United States of America*, **107**, 7095–7100.

Nelson, D.C., Riseborough, J.-A., Flematti, G.R., Stevens, J., Ghisalberti, E.L., Dixon, K.W. *et al.* (2009) Karrikins discovered in smoke trigger Arabidopsis seed germination by a mechanism requiring gibberellic acid synthesis and light. *Plant Physiology*, **149**, 863–873.

Nelson, D.C., Scaffidi, A., Dun, E.A., Waters, M.T., Flematti, G.R., Dixon, K.W. *et al.* (2011) F-box protein MAX2 has dual roles in karrikin and strigolactone signaling in Arabidopsis thaliana. *Proceedings of the National Academy of Sciences of the United States of America*, **108**, 8897–8902.

Osterlund, M.T., Hardtke, C.S., Wei, N. & Deng, X.W. (2000) Targeted destabilization of HY5 during light-regulated development of Arabidopsis. *Nature*, **405**, 462–466.

Oyama, T., Shimura, Y. & Okada, K. (1997) The Arabidopsis HY5 gene encodes a bZIP protein that regulates stimulus-induced development of root and hypocotyl. *Genes & Development*, **11**, 2983–2995.

Scaffidi, A., Waters, M.T., Ghisalberti, E.L., Dixon, K.W., Flematti, G.R. & Smith, S.M. (2013) Carlactone-independent seedling morphogenesis in Arabidopsis. *The Plant Journal*, **76**, 1–9.

Scaffidi, A., Waters, M.T., Sun, Y.K., Skelton, B.W., Dixon, K.W., Ghisalberti, E.L. *et al.* (2014) Strigolactone hormones and their stereoisomers signal through two related receptor proteins to induce different physiological responses in Arabidopsis. *Plant Physiology*, **165**, 1221–1232.

Sentandreu, M., Martín, G., González-Schain, N., Leivar, P., Soy, J., Tepperman, J.M. *et al.* (2011) Functional profiling identifies genes involved in organ-specific branches of the PIF3 regulatory network in Arabidopsis. *The Plant Cell*, **23**, 3974–3991.

Shen, H., Luong, P. & Huq, E. (2007) The F-box protein MAX2 functions as a positive regulator of photomorphogenesis in Arabidopsis. *Plant Physiology*, **145**, 1471–1483.

Shen, H., Zhu, L., Bu, Q.-Y. & Huq, E. (2012) MAX2 affects multiple hormones to promote photomorphogenesis. *Molecular Plant*, **5**, 750–762.

Sokolovsky, V., Kaldenhoff, R., Ricci, M. & Russo, V.E.A. (1990) Fast and reliable mini-prep RNA extraction from Neurospora crassa. *Fungal Genetics Reports*, **37**(1), https://doi.org/10.4148/1941-4765.1492.

Soundappan, I., Bennett, T., Morffy, N., Liang, Y., Stanga, J.P., Abbas, A. *et al.* (2015) SMAX1-LIKE/D53 family members Enable distinct MAX2-

© 2021 The Authors.
The Plant Journal published by Society for Experimental Biology and John Wiley & Sons Ltd.,

dependent responses to strigolactones and Karrikins in Arabidopsis. *The Plant Cell*, **27**, 3143–3159.

Stanga, J.P., Morffy, N. & Nelson, D.C. (2016) Functional redundancy in the control of seedling growth by the karrikin signaling pathway. *Planta*, **243**, 1397–1406.

Stanga, J.P., Smith, S.M., Briggs, W.R. & Nelson, D.C. (2013) SUPPRESSOR OF MORE AXILLARY GROWTH2 1 controls seed germination and seedling development in Arabidopsis. *Plant Physiology*, **163**, 318–330.

Stirnberg, P., Furner, I.J. & Leyser, H.M.O. (2007) MAX2 participates in an SCF complex which acts locally at the node to suppress shoot branching. *The Plant Journal*, **50**, 80–94.

Stirnberg, P., van De Sande, K. & Leyser, H.M.O. (2002) MAX1 and MAX2 control shoot lateral branching in Arabidopsis. *Development*, **129**, 1131–1141.

Sun, X.-D. & Ni, M. (2011) HYPOSENSITIVE TO LIGHT, an alpha/beta fold protein, acts downstream of ELONGATED HYPOCOTYL 5 to regulate seedling de-etiolation. *Molecular Plant*, **4**, 116–126.

Sun, Y.K., Flematti, G.R., Smith, S.M. & Waters, M.T. (2016) Reporter gene-facilitated detection of compounds in Arabidopsis leaf extracts that activate the Karrikin signaling pathway. *Front. Plant Sci.*, **7**, 1799.

Sun, Y.K., Yao, J., Scaffidi, A., Melville, K.T., Davies, S.F., Bond, C.S. *et al.* (2020) Divergent receptor proteins confer responses to different karrikins in two ephemeral weeds. *Nature Communications*, **11**, 1264.

Swarbreck, S.M., Guerringue, Y., Matthus, E., Jamieson, F.J.C. & Davies, J.M. (2019) Impairment in karrikin but not strigolactone sensing enhances root skewing in Arabidopsis thaliana. *The Plant Journal*, **98**, 607–621.

Thussagunpanit, J., Nagai, Y., Nagae, M., Mashiguchi, K., Mitsuda, N., Ohme-Takagi, M. *et al.* (2017) Involvement of STH7 in light-adapted development in Arabidopsis thaliana promoted by both strigolactone and karrikin. *Bioscience, Biotechnology, and Biochemistry*, **81**, 292–301.

Toh, S., Holbrook-Smith, D., Stokes, M.E., Tsuchiya, Y. & McCourt, P. (2014) Detection of parasitic plant suicide germination compounds using a high-throughput Arabidopsis HTL/KAI2 strigolactone perception system. *Chemistry & Biology*, **21**, 988–998.

Tsuchiya, Y., Vidaurre, D., Toh, S., Hanada, A., Nambara, E., Kamiya, Y. *et al.* (2010) A small-molecule screen identifies new functions for the plant hormone strigolactone. *Nature Chemical Biology*, **6**, 741–749.

Umehara, M., Hanada, A., Yoshida, S., Akiyama, K., Arite, T., Takeda-Kamiya, N. *et al.* (2008) Inhibition of shoot branching by new terpenoid plant hormones. *Nature*, **455**, 195–200.

Van Ha, C., Leyva-González, M.A., Osakabe, Y., Tran, U.T., Nishiyama, R., Watanabe, Y. *et al.* (2014) Positive regulatory role of strigolactone in plant responses to drought and salt stress. *Proceedings of the National Academy of Sciences of the United States of America*, **111**, 851–856.

Vandesompele, J., De Preter, K., Pattyn, F., Poppe, B., Van Roy, N., De Paepe, A. *et al.* (2002) Accurate normalization of real-time quantitative RT-PCR data by geometric averaging of multiple internal control genes. *Genome Biology*, **3**, RESEARCH0034.

Villaécija-Aguilar, J.A., Hamon-Josse, M., Carbonnel, S., Kretschmar, A., Schmidt, C., Dawid, C. *et al.* (2019) SMAX1/SMXL2 regulate root and root hair development downstream of KAI2-mediated signalling in Arabidopsis. *PLoS Genetics*, **15**, e1008327.

Wang, L., Wang, B., Jiang, L., Liu, X., Li, X., Lu, Z. *et al.* (2015) Strigolactone Signaling in Arabidopsis Regulates Shoot Development by Targeting D53-Like SMXL Repressor Proteins for Ubiquitination and Degradation. *The Plant Cell*, **27**, 3128–3142.

Wang, L., Xu, Q., Yu, H., Ma, H., Li, X., Yang, J. *et al.* (2020) Strigolactone and Karrikin Signaling Pathways Elicit Ubiquitination and Proteolysis of SMXL2 to Regulate Hypocotyl Elongation in Arabidopsis thaliana. *Plant Cell*, https://doi.org/10.1105/tpc.20.00140.

Waters, M.T., Nelson, D.C., Scaffidi, A., Flematti, G.R., Sun, Y.K., Dixon, K.W. *et al.* (2012) Specialisation within the DWARF14 protein family confers distinct responses to karrikins and strigolactones in Arabidopsis. *Development*, **139**, 1285–1295.

Waters, M.T., Scaffidi, A., Moulin, S.L.Y., Sun, Y.K., Flematti, G.R. & Smith, S.M. (2015) A Selaginella moellendorffii Ortholog of KARRIKIN INSENSITIVE2 Functions in Arabidopsis Development but Cannot Mediate Responses to Karrikins or Strigolactones. *The Plant Cell*, **27**, 1925–1944. https://doi.org/10.1105/tpc.15.00146.

Waters, M.T. & Smith, S.M. (2013) KAI2- and MAX2-mediated responses to karrikins and strigolactones are largely independent of HY5 in Arabidopsis seedlings. *Molecular Plant*, **6**, 63–75.

Wei, C.-Q., Chien, C.-W., Ai, L.-F., Zhao, J., Zhang, Z., Li, K.H. *et al.* (2016) The Arabidopsis B-box protein BZS1/BBX20 interacts with HY5 and mediates strigolactone regulation of photomorphogenesis. *Journal of Genetics and Genomics*, **43**, 555–563.

Xu, D., Jiang, Y., Li, J., Lin, F., Holm, M. & Deng, X.W. (2016) BBX21, an Arabidopsis B-box protein, directly activates HY5 and is targeted by COP1 for 26S proteasome-mediated degradation. *Proceedings of the National Academy of Sciences of the United States of America*, **113**, 7655–7660.

Yao, J., Mashiguchi, K., Scaffidi, A., Akatsu, T., Melville, K.T., Morita, R. *et al.* (2018) An allelic series at the KARRIKIN INSENSITIVE 2 locus of Arabidopsis thaliana decouples ligand hydrolysis and receptor degradation from downstream signalling. *The Plant Journal*, **96**, 75–89.

Yao, R., Ming, Z., Yan, L., Li, S., Wang, F., Ma, S. *et al.* (2016) DWARF14 is a non-canonical hormone receptor for strigolactone. *Nature*, **536**, 469–473.

Zhang, X., Huai, J., Shang, F., Xu, G., Tang, W., Jing, Y. *et al.* (2017) A PIF1/PIF3-HY5-BBX23 Transcription Factor Cascade Affects Photomorphogenesis. *Plant Physiology*, **174**, 2487–2500.

Zhao, L., Peng, T., Chen, C.-Y., Ji, R., Gu, D., Li, T. *et al.* (2019) HY5 Interacts with the Histone Deacetylase HDA15 to Repress Hypocotyl Cell Elongation in Photomorphogenesis. *Plant Physiology*, **180**, 1450–1466.

Zheng, J., Hong, K., Zeng, L., Wang, L., Kang, S., Qu, M. *et al.* (2020) Karrikin signaling acts parallel to and additively with strigolactone signaling to regulate rice Mesocotyl elongation in darkness. *Plant Cell*. Available at:, https://doi.org/10.1105/tpc.20.00123.

Zhou, F., Lin, Q., Zhu, L., Ren, Y., Zhou, K., Shabek, N. *et al.* (2013) D14-SCF (D3)-dependent degradation of D53 regulates strigolactone signalling. *Nature*, **504**, 406–410.

Zoulias, N., Brown, J., Rowe, J. & Casson, S.A. (2020) HY5 is not integral to light mediated stomatal development in Arabidopsis. *PLoS One*, **15**, e0222480.

© 2021 The Authors.